Helsinki University of Technology Doctoral Theses in Materials and Earth Sciences
Espoo 2009 TKK-ME-DIS-9

CHALCOPYRITE DISSOLUTION IN CUPRIC CHLORIDE SOLUTIONS

Doctoral Thesis

Mari Lundström

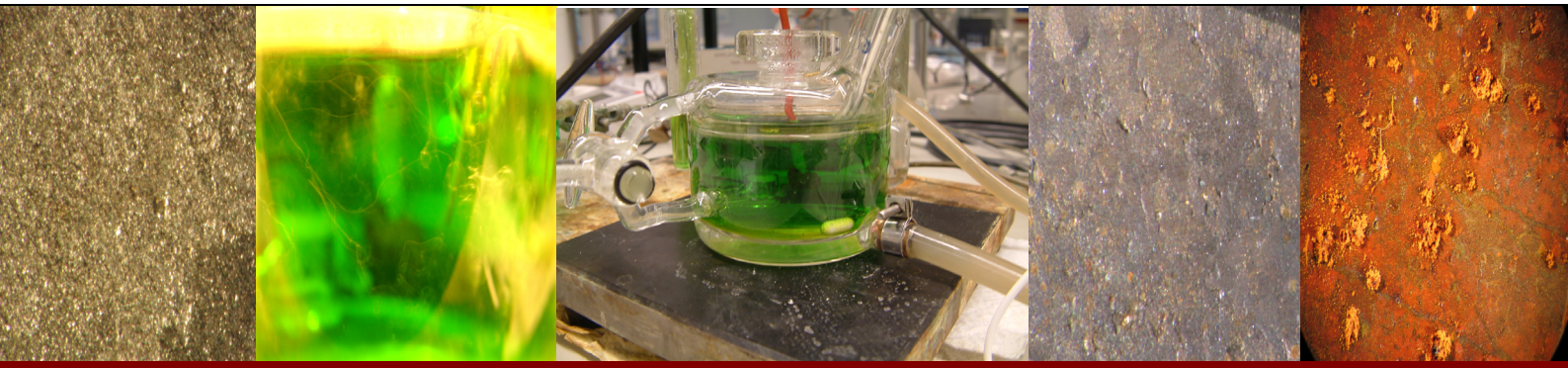

TEKNILLINEN KORKEAKOULU
TEKNISKA HÖGSKOLAN
HELSINKI UNIVERSITY OF TECHNOLOGY
TECHNISCHE UNIVERSITÄT HELSINKI
UNIVERSITE DE TECHNOLOGIE D'HELSINKI

TKK-ME-DIS series
Helsinki University of Technology
Faculty of Chemistry and Materials Sciences
P.O. Box 6200
FIN-02015 TKK

Helsinki University of Technology Doctoral Theses in Materials and Earth Sciences
Espoo 2009 TKK-ME-DIS-9

CHALCOPYRITE DISSOLUTION IN CUPRIC CHLORIDE SOLUTIONS

Doctoral Thesis

Mari Lundström

Dissertation for the degree of Doctor of Science in Technology to be presented with due permission of the Faculty of Chemistry and Materials Sciences, Helsinki University of Technology for public examination and debate in Auditorium 1 at Helsinki University of Technology (Espoo, Finland) on September 25th, 2009, at 12 o´clock noon.

Helsinki University of Technology
Faculty of Chemistry and Materials Sciences
Department of Materials Science and Engineering

Teknillinen korkeakoulu
Kemian ja materiaalitieteiden tiedekunta
Materiaalitekniikan laitos

Distribution:
Helsinki University of Technology
Laboratory of Corrosion and Materials Chemistry
P.O. Box 6200
FIN-02015 TKK, Finland

Available in pdf-format at http://lib.tkk.fi/Diss/

Cover: Polished chalcopyrite sample, Cupric chloride solution, Cell for RDE experiments, Chalcopyrite after leaching at pH 1, Chalcopyrite after leaching at pH 3.

ISBN 978-951-22-9937-9
ISBN 978-951-22-9938-6 (electronic)
ISSN 1795-0074

Multiprint Oy
Espoo 2009

ABSTRACT

Hydrometallurgical technology offers the possibility of processing low-grade or small copper ore bodies and concentrates economically. Chloride solutions have become of great interest, having high leaching kinetics and no passivation of sulfide minerals. This thesis presents an investigation of chalcopyrite ($CuFeS_2$) dissolution in cupric chloride solutions. Firstly, the formation and composition of reaction product layers formed on chalcopyrite were studied. Secondly, the rate-controlling step in chalcopyrite dissolution was defined and thirdly, the prevailing cupric and cuprous species were observed. Electrochemical methods, such as anodic and cathodic polarization, potentiostatic measurements, redox measurements, and electrochemical impedance spectroscopy (EIS) were applied. In addition, stereo-optical microscopy and scanning electron microscopy (SEM) as well as thermodynamic software HSC 5.11/6.1 were used. The solution used had sodium chloride concentrations in the range 250 – 280 g/l, cupric ion concentrations were 0.9 – 40 g/l. The temperature was set to be 70 – 95 ºC and the pH values were in the range of 1 – 3.

The thesis focuses on studying the reaction product layer on chalcopyrite. Color, thickness and the resistance of reaction product layers in the solid – solution interface were determined as a function of time from 0 to 22 hours at pHs 1, 2 and 3. The results suggested that sulfur was present at all times and pHs in the reaction product layers. At pH 1, elemental sulfur was the main phase forming the reaction product layer. This gray colored, porous, and easily removable layer grew to a thickness of 9 μm within 22 hours. The elemental sulfur layer appeared to decrease the rate of the chemical dissolution reaction. By increasing the pH from 1 to 3 and by increasing the dissolution time, the formation of FeOOH became more dominant. At pH 2, the formation of FeOOH was observed after 3 hours and at pH 3 at all leaching times. The co-precipitation of FeOOH was favorable for chalcopyrite dissolution, shifting the dissolution equilibrium to the right. It was determined that the dissolution of a stationary chalcopyrite sample was controlled by diffusion in the reaction product layer at pH 3, changing to chemical rate control at pH 1. FeOOH formation, in addition to the elemental sulfur, favored chalcopyrite dissolution.

In concentrated cupric chloride solutions, cupric ions were assumed to be at least partially not in a chloro-complex form, whereas cuprous ions readily form complexes in chloride solutions. However, cuprous ions were determined not to be chloro-complexed at significantly low cuprous concentrations, in the order of 10^{-13} – 10^{-17} mol/m^3. This was based on the determined E^o value of 0.158 V ± 0.121 V vs. SHE, which is typical for redox couples having cuprous ion not in a chloro-complex form.

TIIVISTELMÄ

Hydrometallurginen teknologia mahdollistaa pienten ja köyhien malmiesiintymien sekä rikasteiden taloudellisen hyödyntämisen. Kloridipohjaisissa liuoksissa sulfidimineraalit liukenevat yleensä nopeasti eivätkä ne tyypillisesti passivoidu. Tässä väitöskirjassa esitetään tutkimustuloksia kalkopyriitin ($CuFeS_2$) liukenemisesta kuprikloridiliuoksissa. Työssä tutkittiin kalkopyriitin pinnalle syntyvien reaktiotuotekerrosten muodostumista sekä niiden koostumusta. Myös kalkopyriitin liukenemista rajoittava tekijä kuprikloridiliuoksessa määritettiin, kuten myös kloridiliuoksessa vallitsevat kupri- ja kupro-osalajit. Tutkimuksissa käytettiin sähkökemiallisia mittausmenetelmiä, kuten anodista ja katodista polarisaatiota, potentiostaattisia mittauksia, redox-potentiaalimittauksia ja sähkökemiallista impedanssispektroskopiaa (EIS). Myös stereo-optista mikroskooppia ja pyyhkäisyelektronimikroskooppia (SEM) sekä termodynaamista laskentaohjelmaa HSC 5.11/6.1 käytettiin. Tutkittu kuprikloridiliuos sisälsi natriumkloridia 250 – 280 g/l ja kupri-ioneja 0.9 – 40 g/l, lämpötila oli 70 – 95 ºC ja pH 1 – 3.

Tutkimuksessa keskityttiin kalkopyriitin reaktiotuotekerrosten tutkimiseen. Kerrosten väriä, paksuutta ja niiden aiheuttamaa vastusta kiinteä – nestepinnan reaktioille tutkittiin ajan (0 – 22 tuntia) ja pH:n (1 – 3) funktiona. Tämän perusteella esitettiin, että reaktiotuotekerroksiin muodostui alkuaineririkkiä kaikissa olosuhteissa. Alhaisilla pH:n arvoilla (pH 1), elementääririkki oli reaktiotuotekerroksen pääfaasi. Tämä harmaa, huokoinen ja helposti irtoava kerros kasvoi 9 µm paksuiseksi 22 tunnin liuotuksen aikana. Kun pH:ta liuotuksessa nostettiin, tuli götiitin (FeOOH) muodostuminen vallitsevaksi. Götiitin muodostuminen havaittiin pH 2:ssa kolmen tunnin liuotuksen jälkeen, kun taas pH 3:ssa FeOOH analysoitiin liuotuksen alusta asti. Götiitin saostuminen siirtää kalkopyriitin liukenemisreaktion tasapainoa reaktiotuotteiden suuntaan, minkä johdosta kemiallisen liukenemisreaktion nopeus kasvoi. Kalkopyriittielektrodin liukenemista rajoittava tekijä määritettiin pH 3:ssa olevan diffuusion reaktiotuotekerroksessa, pH 1:ssä reaktio muuttui kemiallisen reaktion kontrolloimaksi. Götiitti-elementääririkkikerros rajoitti kalkopyriitin liukenemista vähemmän kuin pelkkä elementääririkkikerros.

Väkevissä kuprikloridiliuoksissa kupri-ionin ehdotettiin olevan ainakin osittain kompleksoitumatta, ionimuodossa, kun taas kuproioni on hyvin stabiili klorokompleksina. Tästä huolimatta havaittiin, että hyvin alhaisilla, suuruusluokkaa 10^{-13} – 10^{-17} mol/m^3 olevilla kupropitoisuuksilla, myös kuproioni voi pysyä kompleksoitumattomana, ionimuodossa. Tämä määritys perustui laskettuun E^o:n arvoon 0.158 V ± 0.121 V vs. SHE, mikä on tyypillinen redox-pareille, joissa kuproioni ei ole kompleksoitunut kloridi-ionien kanssa.

PREFACE

The research work presented in this thesis was carried out at Helsinki University of Technology (TKK), Laboratory of Corrosion and Materials Chemistry during the years 2004–2008. I am most deeply grateful to my supervisor Jari Aromaa D.Sc. (Tech), who tirelessly shared the scientific challenges as well as his extensive knowledge with me. His heart is open to students and new unconventional scientific approaches. I would like to express my sincere gratitude to my Professor Olof Forsén for his technical and psychological guidance and support during these years. Both as a professor and a human being, Prof. Forsén is unique.

The thesis is a part of a study carried out in the Graduate School on New Materials and Processes (2006–2008) and would not have been possible without the support of support of the Outokumpu Foundation (2004–2005), Outotec, Tekniikan Edistämissäätiö (TES) and the Otto A. Malm foundation. All financial supporters are greatly acknowledged. I am truly grateful to Michael H. Barker Ph.D. (Tech) for the time and enormous amount of ideas he has shared. I would like to thank Olli Hyvärinen D.Sc. (Tech) and Professor Pekka Taskinen for guiding me in the world of hydrometallurgy and for being my scientific godfathers. Further, I want to express my thanks to Professors Lauri Holappa and Heikki Jalkanen.

I want to thank Robert von Bonsdorff Lic.Sc. (Tech) for the peer-support and the unforgettable conference trips and Anja Talo Lic.Sc. (Tech) for her advice during the first few years. I am also truly grateful to the staff of our laboratory for the pleasant working atmosphere, especially Jorma Virtanen Lic.Sc. (Tech), Antero Pehkonen D.Sc. (Tech), Istvan Galfi M.Sc (Tech), Teppo Salo M.Sc (Tech) and Lauri Pajunen Lic.Sc. (Tech). I would also like to thank Anna Suntio and Mari Karonen for their assistance in conducting some experiments.

I would also like to thank Liisa Haavanlammi M.Sc. (Tech) and Janne Karonen M.Sc. (Tech) for trusting me and for continuing the work Olli started. I would like to thank Jarkko Partinen D.Sc. (Tech) for the co-operation and Mikko Ruonala Lic.Sc. (Tech) for his support. Thanks to Marika Tiihonen M.Sc. (Tech) for sharing her valuable ideas about the HydroCopper® process. Thanks also go to Kari Hietala M.Sc. (Tech) and Martti Nurmisalo M.Sc. (Tech).

I am deeply grateful to my friends supporting me. I also want to thank my workmates at Outotec. Specifically, I want to express my deep gratitude to my current workmate Elli Miettinen D.Sc. (Tech), a former fellow student and a good friend, for her priceless support.

Finally, I am humbly grateful to my parents Juho and Anneli for their support during all the past years. Also the support and love from my sisters Hanna and Paula, their families and Jarkko´s close relatives, are deeply appreciated.

The enormous support, love and flexibility from my great husband Jarkko and my daughter Minea have been invaluable. This thesis is nothing compared to you. This is all a great gift from God.

Espoo, March, 2009 Mari Lundström

CONTENTS

LIST OF PUBLICATIONS

[I] Lundström, M., Aromaa, J., Forsén, O., Hyvärinen, O., Barker, M.H., Leaching of Chalcopyrite in Cupric Chloride Solution. Hydrometallurgy 77(2005), pp. 89-95.

[II] Lundström, M., Aromaa, J., Forsén, O., Hyvärinen, O., Barker, M.H., Cathodic Reactions of Cu^{2+} in Cupric Chloride Solution. Hydrometallurgy 85(2007), pp. 9-16.

[III] Lundström, M., Aromaa, J., Forsén, O., Barker, M.H., Reaction Product Layer on Chalcopyrite in Cupric Chloride Leaching. Canadian Metallurgical Quarterly 47(2008) 3, pp. 245-252.

[IV] Lundström, M., Aromaa, J., Forsén, O., Redox Potential Characteristics of Cupric Chloride Solutions. Hydrometallurgy 95(2009), pp. 285-289.

[V] Lundström, M., Aromaa, J., Forsén, O., Transient Surface Analysis of Dissolving Chalcopyrite in Cupric Chloride Solution. Canadian Metallurgical Quarterly 48(2009) 1, pp. 53-60.

Through the Thesis, the above-mentioned articles will be referred by their Roman numerals.

AUTHOR´S CONTRIBUTION

The research presented in this thesis was carried out at the Helsinki University of Technology in the laboratory of Corrosion and Materials Chemistry as a post-graduate student during the years 2004 – 2009. From 2004 to 2005, the main supporter was the Outokumpu Foundation and from the beginning of 2006 the research was carried out under the auspices of the Graduate school on New Materials and Processes. The support of Tekniikan Edistämissäätiö (TES) and Otto A. Malm´s foundation is also greatly appreciated.

The author has been the main author of all the articles [I–V]. The author wrote all papers [I–V] and the experimental part was mainly carried out by the author as well. The author carried out all the processing of the experimental data. Jari Aromaa (Docent, D.Sc.Tech) has been the main scientific advisor for the author – he has shared numerous scientific discussions and advice, when making the research plan, experiments, and interpreting the experimental results. Professor Olof Forsén, Michael H. Barker (Ph.D.) and Olli Hyvärinen (Docent, D.Sc.Tech) have actively advised the author as well.

In papers I, II, III and V, the author carried out all the electrochemical experimental work herself. SEM analyses and X-ray analyses were carried out by the professional staff at Outotec Research Oy, Pori (paper I, II, V) and Helsinki University of Technology, laboratory of Metallurgy (paper III). In paper IV, the experimental practice was carried out by trainees Mari Karonen and Anna Suntio.

The author took the main responsibility for the study throughout the research. The author has also presented the results covered in this thesis at several international conferences. The author has also published several other articles in this field in non-reviewed journals.

SYMBOLS AND ABBREVIATIONS

A	Electrode area (cm^2)
C	Concentration (mol/L, mol/cm^3, g/l)
d	Thickness (μm)
D	Diffusion coefficient (cm^2/s)
E	Equilibrium potential, redox potential (V, mV)
E^o	Standard electrode potential (V, mV)
Ea	Activation energy (kJ/mol)
E_{pa}	Anodic peak potential (V, mV)
E_{pc}	Cathodic peak potential (V, mV)
ΔE_p	Peak potential separation (V, mV)
F	Faraday´s constant (96485 C/mol)
i_0	Exchange current (A)
I_d	Diffusion current (A)
I_k	Charge transfer current (A)
I_p	Peak height (A)
j_0	Exchange current density (mA/cm^2, A/cm^2)
j_{lim}	Limiting current density (mA/cm^2, A/cm^2)
k^0	Electron transfer rate constant (cm/s)
k_T	Unit rate constant (cm/s)
Q_1	Non-ideal apparent double layer capacitance (Ωcm^2)
Q_2, Q_3	Non-ideal capacitance associated with the reaction product layer (Ωcm^2)
R	Gas constant (J/mol×K)
Rs	Solution resistance (Ω)
R_1	Apparent charge transfer resistance (Ωcm^2)
R_2, R_3	Resistance associated with the reaction product layer (Ωcm^2)
t	Time (s, h)
T	Temperature (K, ºC)
z, n	Number of electrons involved in the reaction
($\gamma_\pm$)	Mean activity coefficient
v	Kinematic viscosity (cm^2/s)
υ	Sweep rate (V/s, mV/s)
ω	Angular frequency (1/s = $2\pi f$)
Ag/AgCl	Silver/silver chloride reference electrode
CE	Counter electrode
EDS	Energy dispersive spectrometer
EIS	Electrochemical impedance spectroscopy
GC	Glassy carbon
LME	London Metal Exchange
OCP	Open circuit potential
RDE	Rotating disc electrode
Redox	Reduction oxidation
REF	Reference electrode
SEM	Scanning electron microscopy
SHE	Standard hydrogen electrode
WE	Working electrode
XRD	X-ray diffraction

1 INTRODUCTION

The development of hydrometallurgical process options for sulfide minerals is of great importance, especially from an environmental viewpoint. As sulfur dioxide emissions from the pyrometallurgical industry are highly undesirable, there is a need to develop economically beneficial processes that convert the sulfur coming from the sulfide minerals into elemental form. Hydrometallurgical processes can also operate profitably in small-scale plants. The possibility to use low-grade concentrates, to achieve low energy consumption, and the ability to regenerate leaching solutions increase the importance of research in this field.

Chalcopyrite, $CuFeS_2$, is the most common copper mineral available in large quantities. Although being the most important copper mineral, chalcopyrite has been observed to be refractory under hydrometallurgical conditions. It has a tetragonal structure in which each sulfur ion is surrounded by four iron or copper ions. The chemical formula of chalcopyrite has been suggested to be $Cu^{+}Fe^{3+}(S^{2-})_2$. In natural copper sulfides however, it is known that the structure of the mineral can more resemble an alloy than a salt and the valences do not correspond to the normal valences of the metal. Part of the sulfur content of copper sulfides can be paired to form S_2^{2-} ions and the solid can be a diamagnetic metallic conductor. [1-3]

In the search for hydrometallurgical alternatives to copper smelting, the leaching of chalcopyrite with sulfuric acid, in combination with various oxidizing agents, has received most of the attention. Processes such as Activox, Nenatech, Dynatec, AAC/UBC, Placer Dome process, Biocop, Bactech/Mintek and Geocoat are nowadays the main sulfate processes for chalcopyrite leaching. Also, Galvanox is currently receiving industrial testing [4, 5]. Sulfate-based processes have certain advantages due to its generally simpler and better-understood chemistry. Metal recovery in sulfate media is well known solvent extraction – electrowinning (SX-EW) technology. However, chloride-based processes are of increasing interest. Chloride leaching has several advantages compared with the sulfate leaching of copper sulfides. Faster leaching kinetics of sulfide minerals in chloride solutions makes it possible to use atmospheric leaching. High dissolution rates enable the use of smaller solution volumes in subsequent steps. Almost all of the sulfur can be oxidized to the elemental form [6]. Chalcopyrite has been shown to be less refractory for leaching in chloride solutions. One challenge in chloride media is the need for special construction materials due to the corrosive nature of chloride solutions. [4, 7-9]

Roman et al. [9] mentioned that as early as 1882 Dortsch and Frochlich were leaching CuS with ferric chloride. In 1923, a ferric chloride leaching process was patented in the U.S, as referred to by Lin [10]. In 1974 Cominco Ltd patented a copper hydrometallurgy ferric chloride leach process that which reduces cuprous ions by using hydrogen [11]. The most favored lixiviant in chloride-based processes has been $FeCl_3$ but $CuCl_2$, BrCl and some combination of these have also been of interest. Applications using cupric chloride are increasing due to the higher oxidation potential and faster dissolution kinetics in cupric chloride solutions when compared to ferric chloride. The main chloride processes have been CLEAR (1976-1982), CYMET, Cuprex, Intec and HydroCopper®, from which CLEAR, CYMET, Intec and HydroCopper® use cupric ions as the oxidant [4]. Several laboratory studies for copper sulfide leaching have also been carried out using cupric chloride solutions

[4, 12-17]. Recently, one of these cupric chloride based processes, HydroCopper®, has reached the commercial scale [18-24]. The HydroCopper® process is described in section 1.3.

1.1 Dissolution of sulfide minerals

Hydrometallurgical methods can be used to produce copper from sulfide minerals, such as chalcopyrite $CuFeS_2$, bornite Cu_5FeS_4, chalcocite Cu_2S and covellite CuS. Generally, leaching of sulfide minerals is carried out in an oxidative environment. In oxidative leaching, there is an oxidizing agent present and electron transfer involved in the dissolution reaction. In an electrochemical process both oxidation and reduction reactions occur. The anodic (oxidation) reaction is most likely the oxidation of sulfur in the sulfide mineral. Simultaneously, the cathodic reaction is the reduction of an oxidizing agent, which is eager to take electrons. The most commonly used oxidizing agents are oxygen, Fe^{3+} (ferric ions), nitric acid, concentrated H_2SO_4 and Cu^{2+} (cupric ions). In oxidative leaching, the leaching media can be either acidic or basic. Solutions are generally based on sulfate, chloride, nitrate, ammonia, or cyanide.

In cupric chloride solutions, the anodic reaction is the dissolution of chalcopyrite, bornite, covellite, chalcocite or other sulfide minerals. The cathodic reaction can be the reduction of cupric ion Cu^{2+}, but also the reduction of cupric complexes, such as $[CuCl]^+$, $[CuCl_3]^-$ and $[CuCl_4]^{2-}$. When a complex concentrate is used, there are numerous reduction-oxidation couples (redox couples), which will determine the equilibrium in the solution. The redox potential of a solution describes its ability to oxidize minerals. A high concentration of oxidants increases the redox potential, whereas the dissolution of sulfide minerals, which reduce the oxidizing agents, decreases the redox potential of a solution. It is known that the redox potential of Cu^{2+}/Cu^+ in chloro-complex form is remarkably high [IV]. This provides a large driving force for the dissolution of sulfide minerals. On laboratory scale, when the concentrations of chemicals are known, the redox potentials can be used to determine concentrations or even standard electrode potentials in a system [IV].

The formation of a reaction product layer is characteristic for sulfide minerals during leaching. This layer is often suggested to be of elemental sulfur, since the sulfur in the sulfide mineral is oxidized to elemental sulfur by the oxidant in the solution. The elemental sulfur layers can decrease the reactivity of the mineral by hindering the dissolution of oxidants to the reacting mineral surface or metal cations transfer from the sulfide mineral to the solution.

1.2 Chloride solutions

In hydrometallurgical applications the use of chloride solutions instead of sulfate solutions is becoming more common. Generally, metal ions in water solutions are present as aqua ions, such as $Cu(H_2O)_6^{2+}$ (in this thesis referred as Cu^{2+}). In chloride solutions, however, chloride ions are actively displacing water molecules in the coordination spheres of many metal ions forming chloro-complexes [25]. The advantage of chloride solutions is the aggressive nature of the leaching and the stability of the Cu^+, cuprous ion, in a chloro-complex form. Cuprous ions also form stable complexes with ammonia, bromide, iodide, thiocyanate, sulfite, thiosulfate, cyanide and a number of organic chelating reagents. Most metals are highly soluble in salt solutions due to complexation with chloride ions [20]. Specifically, leaching of sulfides occurs more easily in chloride than in sulfate solutions because the activation energy for leaching in chloride solutions is lower compared to sulfate solutions [26]. The

conductivity of chloride solutions is high and electrochemical reactions are highly reversible. Also, the potential series of metals in chloride solutions are different from the standard ones. [13, 27]

Both the Fe^{3+}/Fe^{2+} and Cu^{2+}/Cu^{+} redox potentials are higher in chloride solutions compared to sulfate solutions. Fe^{3+} forms strong complexes with the sulfate in sulfate solutions, lowering the activity of the oxidant. In chloride solution the complexation of Fe^{3+} is not as strong and the oxidant has a higher activity. In cupric chloride leaching, Cu^{+} forms very strong complexes with chloride ions, increasing Cu^{2+} activity. Also, the redox potential of Cu^{2+}/Cu^{+} is higher than that of Fe^{3+}/Fe^{2+} in concentrated chloride solutions. This makes the dissolution more advantageous in cupric chloride solutions compared to ferric chloride solutions [28]. It has also been shown that the addition of cupric chloride to ferric chloride leaching promotes chalcopyrite dissolution [29]. The ability of chloride ions to form complexes is very important. Berger et al. [30] proposed the following classification of the strength of Cl^- acceptors: $AgCl > CuCl > PbCl_2 > ZnCl_2 > CuCl_2 > FeCl_3 > FeCl_2 > NiCl_2 > HCl, NaCl, KCl$ (Cl^- donors).

Cuprous chloride is sparingly soluble in water [31], however, in concentrated chloride solutions higher solubilities can be achieved [27]. The cation of the added chloride salt can also affect the solubility. The solubility of CuCl can be defined in two ways in a CuCl-NaCl-H_2O system: at high copper concentrations CuCl precipitation defines the solubility limit (at 75 °C with [NaCl] = 250 g/l the limit is ca. 270 g/l) and at a high NaCl concentration, the solubility is defined by NaCl precipitation, at 75 °C with [CuCl] = 30 g/l the limit is ca. 330 g/l [30].

Cupric chloride is highly soluble in water [9, 31]. The solubility of Cu(II) decreases with increasing Cl^- concentration. This is the opposite of cuprous chloride. There have been a number of studies on the solubility of Cu(II) at different temperatures. It has been shown that for Cl^- concentrations below 4 mol/kg there is no strong effect on Cu(II) solubility at 50 ˚C, but at Cl^- concentrations >4 mol/kg the solubility of cupric ions decreases considerably [30].

Experimental studies and thermodynamic calculations have been carried out on the complexes present in a copper chloride media [30, 32-41]. It is generally agreed that in aqueous solutions Cu^{+} and chloride ions form a series of complexes $[CuCl_n]^{1-n}$, where $n \leq 4$ [40]. There is less of a consensus about the complexation of cupric ions, since the prevailing cupric species has been suggested to be both cupric ion and its chloro-complex. [38, 42, 43]. In concentrated cupric chloride solutions, the mean activity coefficient ($\gamma_{\pm}$) values in the presence of sodium chloride are relatively high. With a 4 mol/kg NaCl solution at 90 °C $\gamma_{\pm}$ for NaCl is 0.763. The $\gamma_{\pm}$ of $CuCl_2$ has not been reported at 90 °C, but the $\gamma_{\pm}$ value at 25 °C is 0.398 with $[CuCl_2]$ = 0.7 mol/kg [44]. This non-ideal behavior of concentrated cupric chloride solutions makes the thermodynamic observations complicated.

1.3 HydroCopper® process

HydroCopper®, which covers the technology for leaching sulfide minerals in cupric chloride solutions in combination with solution purification and cuprous oxide precipitation, has been trademarked and registered by Outotec Oyj. It is a cupric chloride leaching process based on the good leaching properties of sulfide minerals in cupric chloride solution. One major advantage of HydroCopper® is that almost all the sulfur can be oxidized into elemental form.

This has not been evident in the hydrometallurgical processes studied earlier, due to the formation of sulfuric acid [45]. The possibility to recover precious metals, such as gold and silver from the concentrate makes the process more efficient than sulfuric acid leaching.

HydroCopper® is operated at normal pressure and at a temperature of 80-100 ˚C using stirred reactors, thickeners and other conventional hydrometallurgical equipment. The raw material is copper sulfide, preferably chalcopyrite concentrate, which is leached in a chloride solution by Cu^{2+}. Generally, the dissolution reactions decrease the pH of the solution. The pH is kept between 1.5 and 2.5 with the oxygen feed to the leaching reactors. If the oxygen-feed is too high, then the pH tends to rise causing precipitation of copper hydroxychloride (atacamite). Too low a pH favors the formation of jarosite ($MFe_3(SO_4)_2(OH)_6$, where M = K, Na, NH_4, Ag, etc). *Figure 1* presents a general process flow diagram of the HydroCopper® process. A typical retention time for the concentrate is 10-20 hours.

Chalcopyrite can be oxidized in a chloride solution with the help of Cu^{2+} ions according to the reaction (1).

$$CuFeS_{2(s)} + 3Cu^{2+}{}_{(aq)} \rightarrow 4Cu^{+}{}_{(aq)} + Fe^{2+}{}_{(aq)} + 2S^{0}{}_{(s)} \quad (1)$$

Additionally, in the presence of oxygen, cuprous ions can be partially oxidized to cupric and ferrous to ferric. Ferrous ions can also reduce cupric ions to give ferric and cuprous. Ferric ions are then precipitated as goethite or akaganeite (FeOOH) or hematite (Fe_2O_3). The overall reaction can be described, for example, by reaction (2).

$$CuFeS_{2(s)} + Cu^{2+}{}_{(aq)} + 3/4O_{2(g)} + ½\ H_2O_{(l)} \rightarrow 2Cu^{+}{}_{(aq)} + FeOOH_{(s)} + 2S^{0}{}_{(s)} \quad (2)$$

The other base metal sulfides present in the concentrate (Zn, Pb, Ni, Ag) are dissolved into the solution e.g. by the reaction (3).

$$ZnS_{(s)} + 2Cu^{2+}{}_{(aq)} \rightarrow Zn^{2+}{}_{(aq)} + 2Cu^{+}{}_{(aq)} + S^{0}{}_{(s)} \quad (3)$$

In equations (1) – (3) Cu^{+} and Cu^{2+} represent the general oxidation state of the copper species and not the exact solution species, since copper ions may also be present in complex form.

After the sulfides dissolve, oxygen purging increases the redox potential in the solution enabling the gold leaching as chloro-complexes. Gold is leached at potentials >0.800 V vs. SHE and recovered from the solution by precipitating it on activated carbon or copper concentrate [24, 46]. The solution from the first leaching stage of the HydroCopper® process contains about 70 g/l copper, of which 60 g/l is Cu^{+} and 10 g/l is Cu^{2+}. The second and third leaching stages are more oxidative and the concentration of cupric copper is higher. The solution purification section consists of five stages: cupric removal, silver removal by cementation, neutralization in which zinc and lead are removed, ion exchange with impurity removal and Cu_2O precipitation. Cu_2O precipitation is carried out with sodium hydroxide (4), which is produced by the chlor-alkali electrolytic cell.

$$2CuCl_{(s)} + 2NaOH_{(aq)} \rightarrow Cu_2O_{(s)} + 2NaCl_{(aq)} + H_2O_{(l)} \quad (4)$$

The formation of cuprous chloro-complexes makes it possible for the HydroCopper® process to produce high-grade copper. This is due to the fact that cuprous chloro-complexes are very

stable in solution, and precipitate only at pHs >9. Cupric ions readily precipitate at pH 3-4 and zinc and lead ions at pH 6-7. Minor impurities can also be separated from the cuprous chloride solution in the ion exchange stage. Thus all other impurities can be efficiently precipitated or purified in the ion exchange and high grade cuprous oxide precipitated.

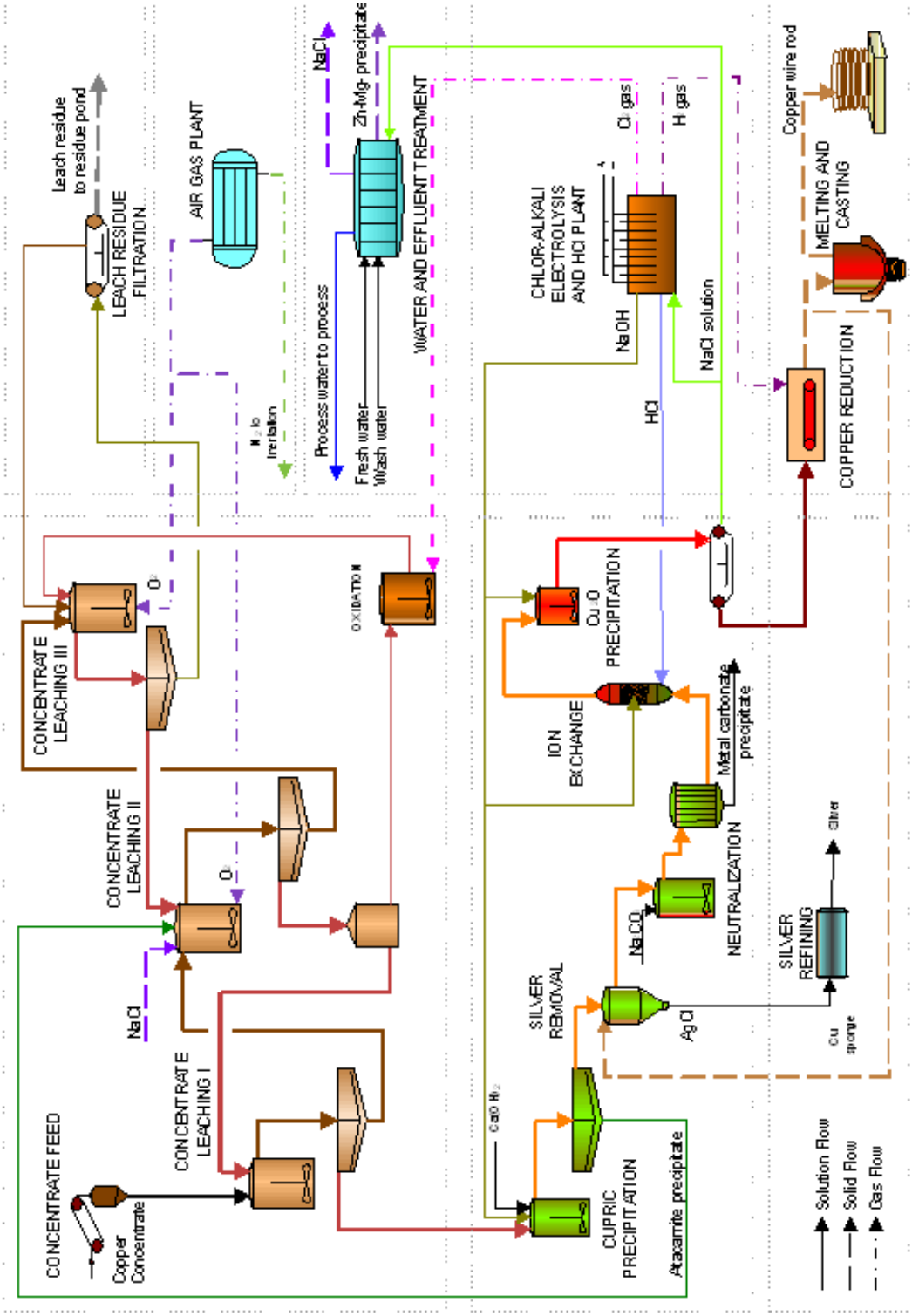

Figure 1. *General process flow diagram of the HydroCopper® process. [47]*

The intermediate product, cuprous oxide, is precipitated as a powder with a particle size of 50-80 microns. The slurry from the precipitation reactors is washed and filtered on a vacuum belt filter. *Figure 2* shows chalcopyrite concentrate feeding to the process and the intermediate product cuprous oxide on the belt filter. The sodium chloride filtrate is recycled to the chlor-alkali electrolysis, where the regeneration of chemicals occurs. The filter cake is fed into a belt furnace, in which the cuprous oxide is dried and reduced to LME grade metallic copper at 650-850 °C (Reaction 5).

$$Cu_2O_{(s)} + H_{2(g)} \rightarrow 2\ Cu_{(s)} + H_2O_{(g)} \quad (5)$$

Figure 2. *Chalcopyrite concentrate feeding from the conveyor to the concentrate pulp tank (left) and cuprous oxide on the belt filter (right) at the Outotec Research HydroCopper® demo plant, Pori, Finland.*

The reduced copper plates that are formed are charged into the melting furnace, where molten copper is deoxidized with a graphite layer over the melt. The copper quality is excellent, meets well the quality measures for a copper feed to a casting unit, and thus can be cast into any form. [18-20, 23, 48].

The experimental research in this thesis [I] – [V] has been carried out under conditions similar to those used in the HydroCopper® process. Additionally, several other laboratory-scale studies have been published in the HydroCopper® type of environment. [42, 46, 49-52]

1.4 Scope of the thesis

This study is a part of the research carried out in the HydroCopper® environment. The hypothesis in section 1.4.1 presents the starting point for the study – the assumed characteristic behavior for chalcopyrite and concentrated cupric chloride solutions. It needs to be mentioned that this study was not a part of the HydroCopper® process development, but focused on studying certain scientifically interesting phenomena in concentrated cupric chloride solutions, the structure being presented in section 1.4.2, and the new results in section 1.4.3.

1.4.1 Hypothesis

The leaching of chalcopyrite in cupric chloride solutions, near to the boiling point of the solution, is electrochemical in nature - there are electron transfer reactions involved in the dissolution process. As chalcopyrite is exposed to concentrated cupric chloride solution, the anodic reaction is oxidation of sulfur from the chalcopyrite lattice. The anodic dissolution reaction demands a simultaneous cathodic reduction reaction. The cathodic reaction is the reduction of cupric ions or chloro-complexes to cuprous ions or chloro-complexes. Cuprous and cupric ions readily form complexes, thus cupric and cuprous species in solution are likely to be present in a chloro-complex form.

During chalcopyrite leaching in cupric chloride solution, a reaction product layer forms on the chalcopyrite surface. Commonly, this layer has been suggested to be elemental sulfur [16, 17]. The composition of the reaction product layer is strongly affected by the pH of the process solution. As the reaction product layer grows with time, it can limit the diffusion of oxidants to the chalcopyrite surface or hinder the diffusion of leached ions away from the surface, thus limiting the rate of the dissolution reaction.

The main objectives of the study were:

i) To determine the composition of chalcopyrite reaction product layers, with respect to pH and leaching time in concentrated cupric chloride solutions. The formation mechanism and thickness of the reaction product layer as a function of time and pH were also of interest. One aim was to measure the electrical properties of the chalcopyrite reaction product layer as a function of time and pH. The reaction product layer was believed to be elemental sulfur, iron compounds or both.

ii) To determine the rate-controlling step for the dissolution of chalcopyrite in concentrated cupric chloride solution. The hypothesis was that the rate-controlling step is diffusion through the reaction product layer.

iii) To specify the cupric and cuprous chloride species present in concentrated cupric chloride solutions.

1.4.2 Structure of the work

The structure of this thesis consists of the introduction and experimental chapters, which are followed by the results concerning the reaction product layer, the rate controlling step, and the species present in the cupric chloride solutions. Prior to the introduction, the abstract, preface and list of publications in the thesis, i.e. papers [I] – [V] are also given. In addition the author's contribution in the publications is clarified.

The introduction presents briefly the history of chloride-based hydrometallurgical processes. The characteristics of sulfide mineral dissolution and chloride solutions are also presented as well as the principles of the HydroCopper® process. The introduction also includes the hypothesis, structure, and new results. Experimental arrangement and procedures are presented briefly after the introduction. Electrochemical methods were used to test the hypothesis, to find the effect of varying the leaching parameters, such as cupric ion concentration, temperature, and pH on the chalcopyrite leaching rate and on the reaction

product layer. A process window was built [I], based on these results. The process window revealed the general trends in chalcopyrite leaching behavior and it was used as the starting point for this research. This process window showed how the electrochemical response of a solid chalcopyrite sample in cupric chloride solution was strongly affected by pH. This process window was also used to determine the leaching conditions for all experiments. Additional information of the experimental detail can be found in publications [I] – [V].

The three theses are each presented as an individual chapters (3 – 5). Each chapter presents the theoretical background for the study, methods and most importantly the results gained in the studied field. Firstly, in chapter 3, the composition of the chalcopyrite reaction product layer and formation of phases as a function of time and pH are clarified. Secondly, chapter 4 reveals the rate-controlling step for the dissolution of chalcopyrite in cupric chloride solutions. Thirdly, the species present in cupric chloride solutions and specifically the standard electrode potential in cupric chloride solution are presented. Finally, the results are discussed in chapter 6. *Figure 3* shows schematically the structure of this work. Each column summarizes the experiments related to a certain thesis (1 – 3) and main the results (1.1, 1.2, 1.3, 2.1, 3.1 and 3.2). Roman numerals refer to the articles in which the experiments were published.

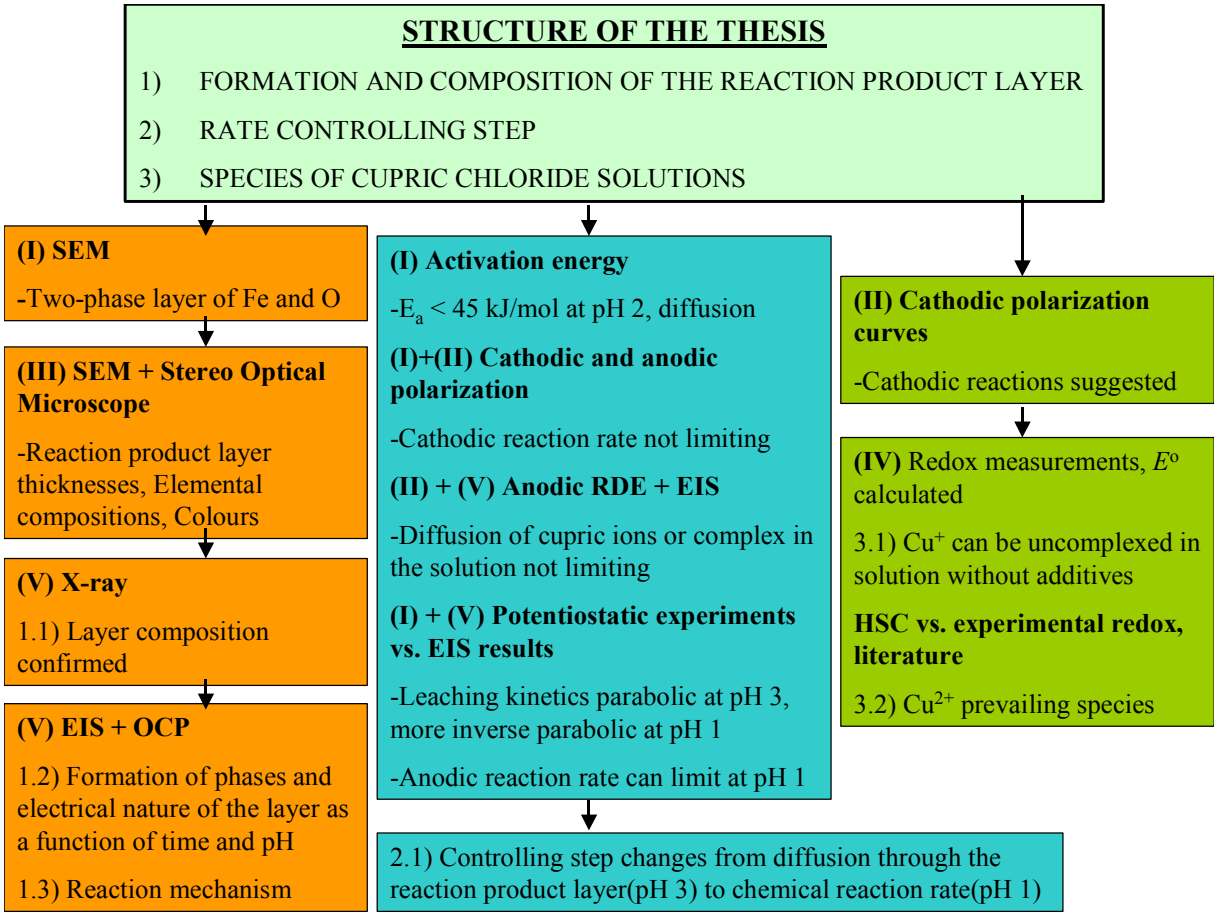

Figure 3. Structure of the thesis, main results (1.1 – 3.2) and experiments related to the results. Roman numerals refer to the articles in which the experiments were published.

1.4.3 New results

The following findings are believed to be original:

i) In a concentrated cupric chloride solution, at temperatures near to the boiling point of the solution, the reaction product layer of a solid chalcopyrite was strongly affected by the pH and leaching time. At low pHs and with short leaching times, the layer was an elemental sulfur layer, but with increasing leaching time and solution pH, FeOOH became dominant. FeOOH formation beside the elemental sulfur favored chalcopyrite dissolution by (i) pushing the chalcopyrite leaching reaction forward and by (ii) making the reaction product layer less hindering for diffusion of solution species.

ii) In concentrated cupric chloride solutions, near to the boiling point of the solution, the rate of dissolution of the chalcopyrite electrode was limited by the diffusion of cupric ions or complexes through the reaction product layer at pH 3 changing into chemical control at pH 1.

iii) In concentrated cupric chloride solution without additives E^o was -0.158 V ± 0.121 V vs. SHE. This indicated that at very low concentrations cuprous ions can remain uncomplexed, i.e. they are not complexed with chloride ions. The species of cupric ion could not be specified, but it suggested that Cu^{2+} can be present at least partially not in a chloro-complex form.

2 EXPERIMENTAL

2.1 Electrodes

The electrode materials used in these studies were chalcopyrite, platinum (Pt) and glassy carbon (GC). The chalcopyrite used to make electrodes was from two sources: the Finnish samples were from the Pyhäsalmi mine, Finland and the North American samples were obtained from a local Finnish gemstone shop. The average Pyhäsalmi copper concentrate mineralogical composition is 74% chalcopyrite, 10% pyrite, 4% sphalerite and 12% others. The average composition of the chalcopyrite in Pyhäsalmi concentrate is Cu 34.3%, Fe 30.4%, S 34.9%, Zn 0.04% and Ag 0.02%. However, no concentrate was used, but the chalcopyrite samples were chosen carefully from the liberated anhedral grains. The chosen chalcopyrite samples were examined both microscopically and visually not to contain other phases on the polished electrode surface. For example, pyrite can be distinguished from the chalcopyrite, which has a more silvery reflection. The average elemental composition of samples used as electrodes was analyzed with SEM/EDS from six Finnish samples (Cu 33.4 ± 0.2%wt, Fe 30.5±0.8%wt and S 36.0±0.7%wt) and eight North American samples (Cu 34.5 ± 0.8%wt, Fe 30.2±0.5%wt and S 35.9±1.0%wt). The analyzed compositions were near to the theoretical composition of chalcopyrite (i.e., Cu 34.6%wt, Fe 30.4%wt and S 34.9%wt). The Pt working electrode was a rod from Radiometer Analytical (France), and was also used as a counter electrode in the rotating disc electrode measurements. GC electrode was a 5-mm disk (Johnson Matthey Type 1, Alfa Aesar, Germany), housed in a PTFE sheath and prepared at Outotec Research Oy (Pori, Finland).

The counter electrode was an in-house made Pt sheet (*Figure 4*) when using a stationary working electode and a Pt rod (Radiometer Analytical, *Figure 5*), when using the rotating disc electrode. The reference electrode in all experiments was Ag/AgCl (REF201, Radiometer Analytical, France), which has a potential of 0.197 V vs. the standard hydrogen electrode (SHE) [53]. The precision of the reference electrode was checked regularly against two other Ag/AgCl electrodes.

2.2 Solutions

The solution used was close to the process solution used in the HydroCopper® process. The concentration of NaCl was 250 g/l or 280 g/l (4.3 M or 4.8 M, respectively). The initial cupric ion concentration varied in the range of 0.1 – 40 g/l. The temperature was between 25 - 90 ˚C and the pH varied between 1 and 3 with the addition of HCl and NaOH. All chemicals were from Riedel-de Haën (Germany), and used without further purification.

2.3 Electrochemical set up

In the experimental work, two electrochemical set-ups were applied. A standard three-electrode electrochemical cell was employed for most of the electrochemical measurements [I, II, III, V]. A schematic diagram of the three-electrode cell is shown in *Figure 6*. When measuring the redox potential of the solution, a two-electrode cell was used [IV].

The vessel was equipped with a thermostated water jacket. In all measurements (except RDE) the cell was stirred with a magnetic stirrer at 500 r.p.m. No purging of gases was done. The working electrode (WE) was a stationary electrode, *Figure 4*, or rotating disk electrode (RDE), *Figure 5*. The counter electrode (CE) was a platinum sheet (*Figure 4* A and B) or a Pt rod (*Figure 5*). The Ag/AgCl reference electrode (REF) was placed in a sintered glass tube containing a gel of agar powder, potassium chloride and distilled water. The reference electrode junction was positioned in an external beaker and connected to the cell via a Luggin capillary. The measurements were carried out using two electrochemical workstations: (i) a PAR 273 Potentiostat/Galvanostat controlled by EG&G PAR´s Model 352 Corrosion Analysis Software 1.00 and (ii) Potentiostat/Galvanostat 2000 working together with a 5050 frequency response analyser (FRA) and 1731 Intelligent/Arbitrary function synthesizer (both NF Corporation, Japan) controlled by in-house software.

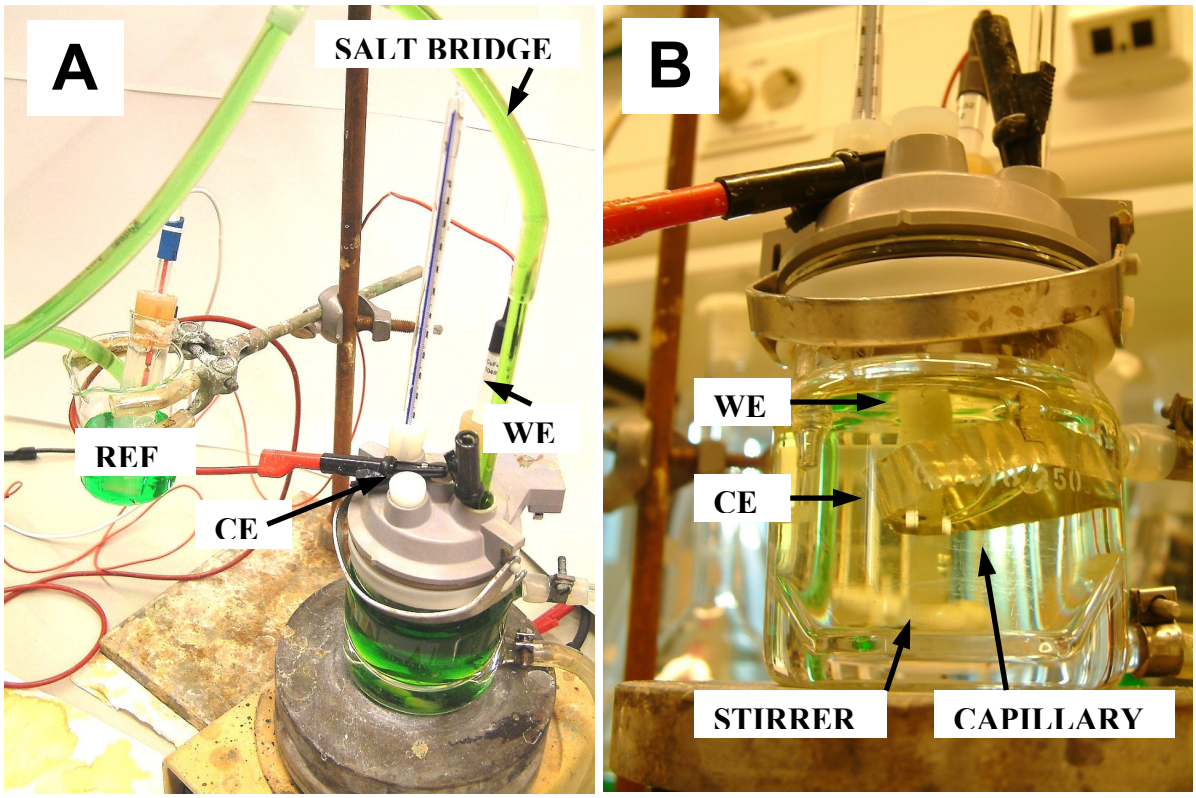

Figure 4 A and B. *The three-electrode cell for a stationary electrode. A) The set up with process solution in the cell. B) The placement of the electrodes and Luggin capillary can be seen more clearly in water.*

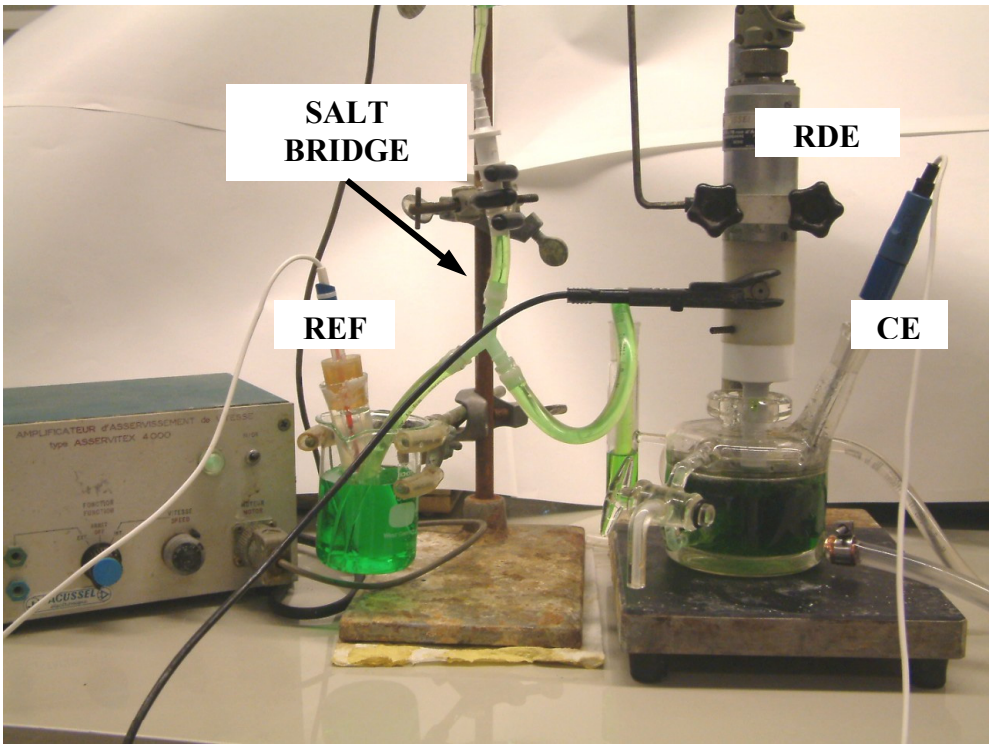

Figure 5. *A three-electrode cell for use with a rotating disk electrode.*

A two-electrode electrochemical cell was employed for redox measurements [IV]. The vessel was equipped with a thermostatic water jacket. The solution was mixed 2 minutes before each of the measurements, but not during the measurements. No purging of gases was done. Two electrodes were used in each measurement - a redox sensor and a reference electrode. The redox sensors used were a glassy carbon disk and a platinum rod as described in section 2.1. The reference electrode was of a type Ag/AgCl. The redox sensor was placed into the cell and the reference electrode was placed in a sintered glass tube containing a gel of agar powder, potassium chloride and distilled water and positioned in an external beaker and connected to the cell via a liquid bridge and a Luggin capillary. The redox measurements were carried out using a digital multimeter (Wavetek 5XL, USA) with an input impedance of 1 MΩ. Physically the cell was the same as shown in *Figure 4*, but only two electrodes were applied.

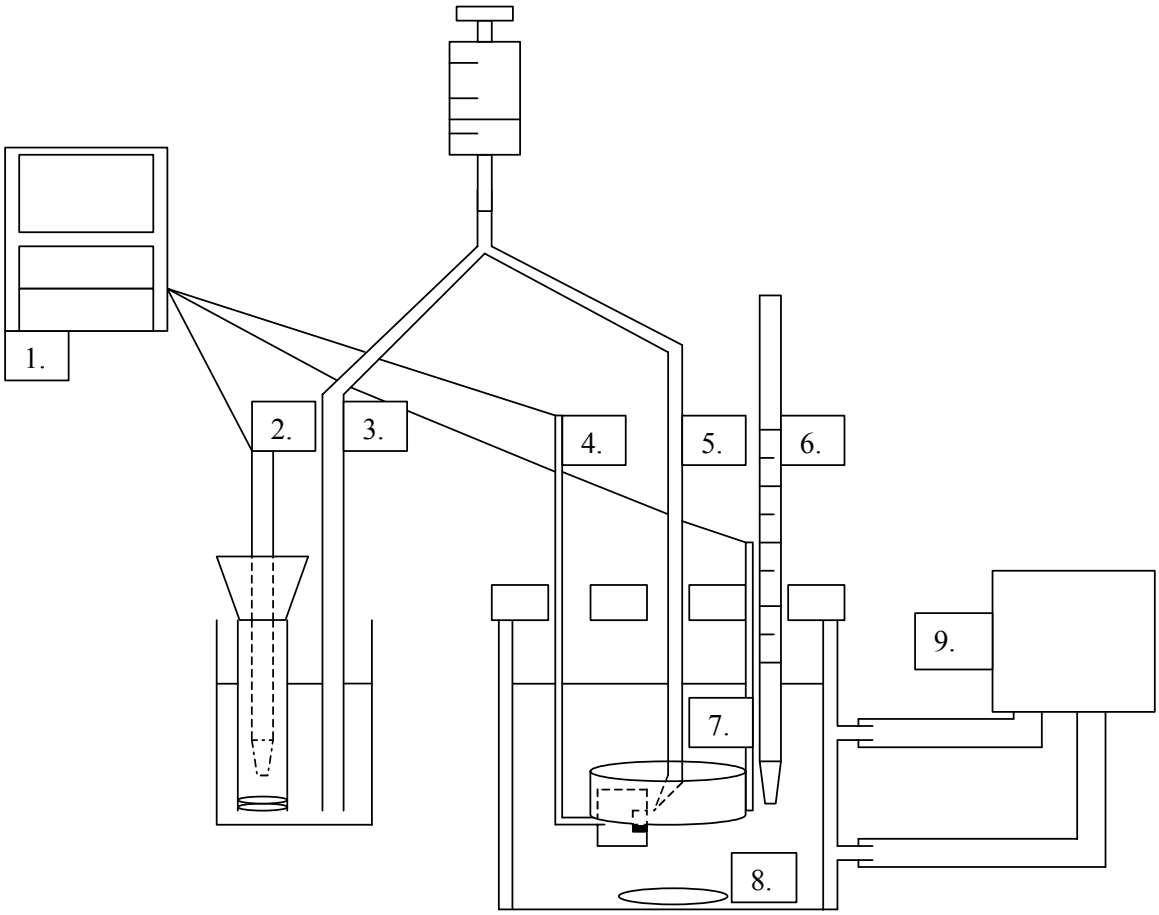

Figure 6. *Schematic diagram of the electrochemical cell used. 1) Electrochemical workstation, 2) Reference electrode (REF), 3) Salt bridge, 4) Working electrode (WE), 5) Luggin capillary, 6) Thermometer, 7) Counter electrode (CE), 8) Magnetic stirrer and 9) Water bath.*

2.4 Procedures

Electrochemical methods, microscopy methods, XRD, thermodynamic calculations and several data analysis techniques were applied in order to test the hypothesis.

By using electrochemical techniques a rapid response of the mineral behavior in a specified environment can be gained. Anodic polarization [I] was applied to define the anodic characteristics of chalcopyrite electrodes. Polarization of chalcopyrite to potentials higher than open circuit potential (OCP) can indicate the possible longer time scale behavior of chalcopyrite at the OCP during the leaching process. Close to the OCP, the corrosion current density and thus the dissolution rate of chalcopyrite were estimated using the Tafel method [I].

By using the RDE technique, the diffusion coefficient of cupric species could also be determined using the Levich equation [I]. In addition, cyclic voltammetry [I,II,III] gives a fast response of the anodic and also cathodic behavior of a material. Potentiostatic measurements [I,III,V] were applied to observe the anodic reaction rates at a defined potential as a function of time. Potentiostatic measurements enable the leaching kinetics and reaction mechanism of chalcopyrite mineral to be observed. Anodic polarization, potentiostatic experiments and cyclic voltammetry revealed the effect of temperature, concentration and pH on chalcopyrite anodic reaction rates. The Arrhenius equation was applied to the anodic polarization data to study the rate reaction controlling mechanism of chalcopyrite dissolution.

Electrochemical impedance spectroscopy (EIS) [III, V] was used to study the chalcopyrite surface and the reaction product layer growing on the mineral. The reaction product layer parameters, such as reaction product layer resistance, reaction product layer capacitance, apparent charge transfer resistance and apparent double layer capacitances were calculated and followed as a function of dissolution time. EIS data were fitted using Boukamps´ software [54].

To determine the elemental and chemical composition of the reaction product layer, SEM/EDS [I, III, V] and XRD [V] were also used. SEM and XRD analyses were carried out at Outotec Research, Pori [I, II, V] and Helsinki University of Technology, Laboratory of Metallurgy [III]. Stereo optical microscopy (Leica MZ6 stereo microscope) was used to observe and photograph chalcopyrite surfaces before and after experiments [I, III, V].

Cathodic reactions in cupric chloride solution were studied using cathodic polarization [II] and exchange current densities were defined by the Tafel method [II]. Cathodic polarization curves were analyzed using the Butler-Volmer equation [II], Koutecky-Levich equation [II] and the method of Nicholson [II].

Thermodynamic software HSC 5.11 and 6.1 (copyright Outotec Research Oy) were applied [I,IV], mainly to study the copper chloro-complexes present in the solution. E^{o} and the form of cuprous species were defined experimentally using redox potential measurements. Data were analyzed using the Nernst equation [IV].

3 FORMATION AND COMPOSITION OF THE CHALCOPYRITE REACTION PRODUCT LAYER

In chalcopyrite leaching, a reaction product layer forms on the mineral surface. If there are particle collisions or a high degree mixing in the leaching reactor, then the reaction product layer can be removed. The reaction product layer on chalcopyrite has conventionally been suggested to be elemental sulfur, a polysulfide (e.g. CuS_2) or an iron precipitate (e.g. ferric oxyhydroxide or jarosite) [55, 56]. On a solid chalcopyrite electrode or in heap leaching, the forming layer can hinder the dissolution of the metal ions into the solution. The passivation of chalcopyrite has caused problems, specifically in sulfate leaching and bioleaching. The slow dissolution kinetics of chalcopyrite has also limited the number of commercial applications of the mineral. In sulfate media, at temperatures below 110 ºC, chalcopyrite is mentioned to leach slowly, having a tendency to accumulate elemental sulfur and iron precipitate product layers, which can hinder the diffusion [57]. It has been shown, however [26], that the addition of sodium chloride to a sulfate solution (0.5 M NaCl, 0.8 M H_2SO_4, T = 95 ºC) changed the amorphous or cryptocrystalline sulfur film into a crystalline and porous sulfur layer that increased remarkably the dissolution rate of chalcopyrite.

The reaction product layer forming in ferric and cupric chloride solutions has generally been suggested to be a more porous sulfur layer, which does not act as a diffusion barrier, but is a less protective and easily removable layer (Table 1). Formation of interference films such as iron oxides has also been observed [58]. In ferric chloride media, iron precipitates as hematite at higher temperatures (>100 °C) and as akaganeite (ßFeO·OH) at lower temperatures [59, 60]. In the presence of hematite seed however, hematite can already form at lower temperatures.

Table 1. Reaction product layers forming on chalcopyrite in ferric and cupric chloride solutions.

LAYER	SOLUTION	TEMPERATURE	SOURCE
Elemental sulfur	0.5 – 1.0 M $FeCl_3$, 1 M HCl	40 – 80 ºC	[61]
Intermediate sulfides	1.0 M $FeCl_3$, 0.2 M HCl	3.5 – 45 ºC	[62]
Amorphous non-stoichiometric, S_4 predominating	0.4 M $FeCl_3$, 1.0 M HCl		[63]
Fine grained sulfur mat with globules and sulfur crystals (8h), sulfur globules with small porosity (24h), partly protective	0.1 M $FeCl_3$, 0.3 M HCl	95 ºC	[64]
Sulfur formation at crystal boundary sites and fractures. Interference films (iron oxides, sulfates) removing sulfur.	0.03 M $FeCl_3$, 0.1 M HCl		[65]
Porous non-protective sulfur	0.02 - 0.50 M $FeCl_3$, 1 M HCl, 3 M NaCl	96 ºC	[66]
Porous elemental sulfur	1.0 M $CuCl_2$, 0.2 M HCl	90 ºC	[16]
Elemental sulfur	0.1– 0.5 M $CuCl_2$, 0.1 M HCl, 4 M NaCl	65 – 104 ºC	[17]

3.1 Stereo-optical microscopy

Twelve cubic chalcopyrite samples (1 cm^3) were leached in a cupric chloride solution [III] for 1, 2, 4 and 22 hours at pHs 1, 2 and 3. The sample surfaces were photographed with a Leica MZ6 stereomicroscope and were later cast in epoxy resin for cross-sectional analysis using the SEM. *Figure 7* shows the photographs of the chalcopyrite surface after leaching for 1 – 22 hours at pHs 1 – 3. It can be seen that at pH 1, the chalcopyrite surface becomes grayer with increasing time, suggesting the presence of elemental sulfur on the mineral surface. At pH 2, the surface becomes more yellow, even brown, with increasing time. At pH 3, the chalcopyrite surface becomes more yellow-orange with increasing time. Goethite (α-FeOOH) has been shown to be a strong yellowish brown, akaganeite (β-FeOOH) a strong brown, lepidocrocite (γ-FeOOH) a moderate orange and hematite (α-Fe_2O_3) a moderate reddish brown [67]. In [III] the presence of FeOOH was suggested. The colors were compared to RAL color cards and published [III] together with estimated reaction product layer thicknesses and compositions.

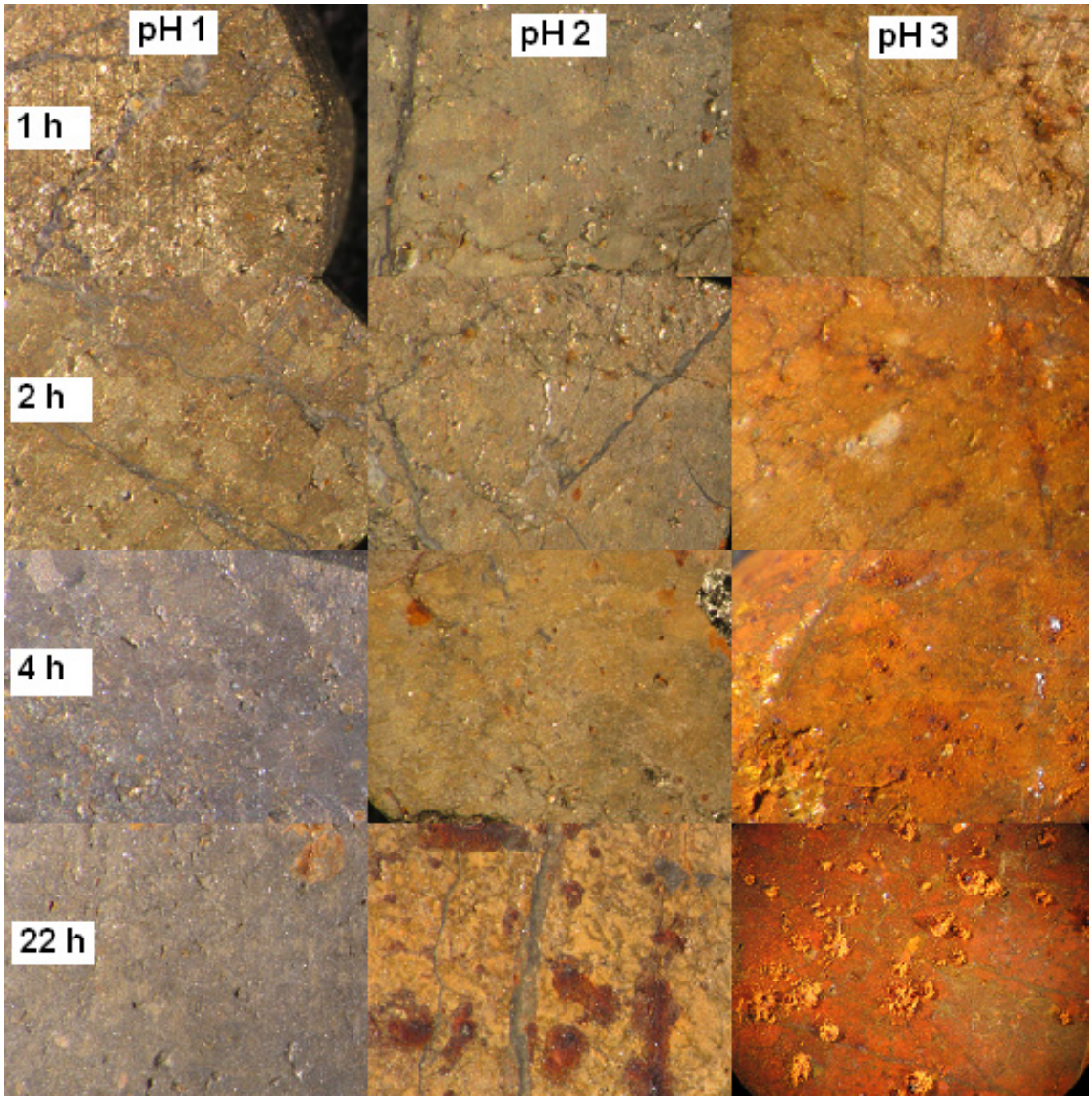

Figure 7. *Reaction product layer color with respect to pH from 1 to 3 and leaching time from 1 to 22 h. The solution had [NaCl] = 280 g/l, [Cu^{2+}] = 30 g/l, T = 90 °C.*

3.2 Scanning Electron Microscopy analyses

Firstly, an SEM analysis was carried out on chalcopyrite electrode surfaces, which had been anodically polarized from OCP to 1.2 V vs. SHE at pH 1.5 and at pH 3 (article [I], figure 4). Also, one cross-sectional analysis was carried out from a polarized sample (Appendix 1). The SEM images were published [52] and can be seen in *Figure 8* and in detail in Appendices 2-4. The samples were analyzed at Outotec Research with a Cambridge S360 scanning electron microscope equipped with an Oxford INCA EDS analyzer. The average EDS analyses from the selected area were presented. The elemental data from EDS included all the elements and their normalized weight percentages. The EDS data were normalized in order to find an empirical formula for the surface composition. The normalized mass of each element was divided by the atomic weight, giving the number of moles in the empirical formula. It must be taken into account that SEM/EDS analyses have a drop shape volume and if the surface layer is thin, it also counts the elements under the reaction product layer. However, the analyzed values before and after the polarization can be compared. The changes in composition can be used to estimate the composition of the surface product layer.

Figure 8 shows the surface before and after polarization at pH 1.5 and 3. It can be seen that before polarization, the mineral composition is near to the theoretical composition of chalcopyrite (Cu:Fe:S was 5:5:11). After polarization at pH = 1.5, a slight excess of sulfur was detected (Cu:Fe:S was 5:5:12). The analysis after polarization at pH = 3 showed a dramatic change in the surface composition, no copper was detected; instead the surface was mainly composed of iron, sulfur and oxygen and (Fe:S:O:Cl was 6:12:13:1). This layer was assumed to be a hematite, goethite, or iron hydroxide type layer [I]. Appendices 2 – 4 show a more detailed analysis of the samples in *Figure 8*.

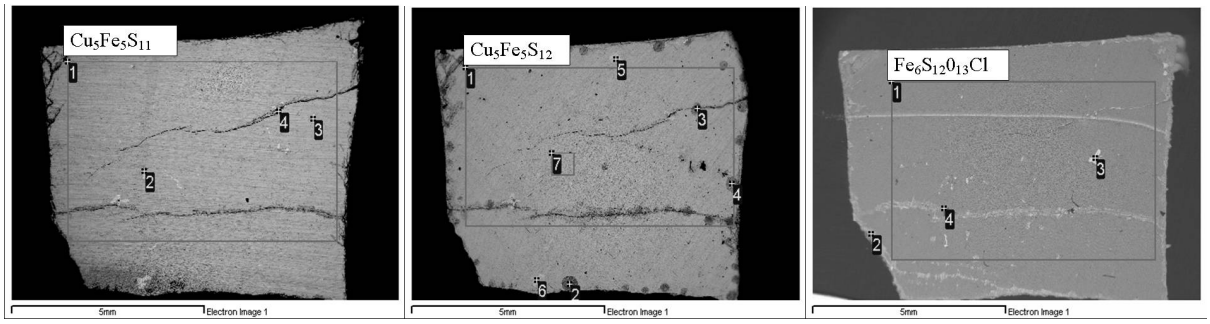

Figure 8. *SEM images of the $CuFeS_2$ electrodes. Ratio of elements (Cu:Fe:S) was 5:5:11 (polished, left) and 5:5:12 (at pH 1.5, middle) when calculated quantitatively from area 1. At pH 3 Fe:S:O:Cl was 6:12:13:1 (right). The solution contained [NaCl] = 250 g/l, $[Cu^{2+}]$ = 17.9 g/l, T = 85 °C. The area analysis of the polished chalcopyrite sample gave Cu = 33.2 wt%, Fe = 30.00 wt% and S = 36.10 wt%, having small sphalerite inclusions (Appendix 2). The area analysis of chalcopyrite dissolved at pH 1.5 gave a sulfur rich analysis Cu = 32.38 wt%, Fe = 29.60 wt% and S = 38.12 wt%, having chlorine – oxygen rich aggregates, sphalerite and silver rich inclusion (Appendix 3). The area analysis of chalcopyrite dissolved at pH 3.0 gave an iron-oxygen rich analysis Cu = 2.48 wt%, Fe = 33.61 wt%, S = 38.76 wt% and 21.41 wt%, having small chlorine excess (Appendix 4).*

The first SEM images (*Figure 8*) showed an indication of excess sulfur at lower pHs and of iron, oxygen and sulfur at higher pHs. The potentials in the anodic polarization experiment

were high (1.2 V vs. SHE). SEM analyses were carried out on the leached samples shown in *Figure 7* [III], in order to define the composition and the thickness of the reaction product layer. A LEO 1450 SEM/Oxford Instruments® INCA EDS was used to analyze the structure and the compositions of the reaction product layer. The samples (*Figure 7*) were mounted in epoxy resin, crosscut, and polished to give a cross-section of the leached surface.

Originally, an elemental analysis of the reaction product layer was carried out using point analysis. Point analyses of the cross-section SEM image were carried out, such as shown in article [III] Figure 6 and Figure 8. However, it was observed that the reaction product layer was only ≤5 μm thick at leaching times ≤4 h, which made it difficult to make a point analysis of the reaction product layer. Also, when polishing the sample leached at pH 1, gray particles were observed in the epoxy and the polishing wheel, indicating that the gray reaction product layer formed at pH 1 was easily removable. For that reason, the line scan was applied such as in article [III] (Figure 7 and Figure 9).

The line scan gave a better indication of the thickness and the composition of the reaction product layer for all samples. The thickness of the layer was determined following the pulse signals – epoxy resin gives either very low signals (as in *Figure 9* at pH 3 for 22 hour) or O and Cl pulses if air bubbles or Cl resins are present (as in *Figure 9* at pH 1 for 22 hours). The base material chalcopyrite gives pulses of S, Fe and Cu. If the chalcopyrite sample was fragile or uneven, the base material did not give even pulses (as in *Figure 9* at pH 2 for 22 h). Between the epoxy and the base chalcopyrite material there was a reaction product layer, which gave pulses of the elements present in the layer. The thickness of the layer was also estimated based on this. It must be noted that the number of pulses does not directly describe the concentration of a certain element, but the trends in the number of pulses indicate if the concentration of an element at a certain point is increasing or decreasing. *Figure 9* shows the line scans of samples at pHs 1, 2 and 3 after 22 hours´ leaching. Line scans were also carried out at each pH after 1, 2 and 4 hours of leaching. The curves on the base materials side from top to bottom are S, Fe, Cu, O and Cl. A more detailed look on the line scans for 22 h at pH 3 was presented in article [III].

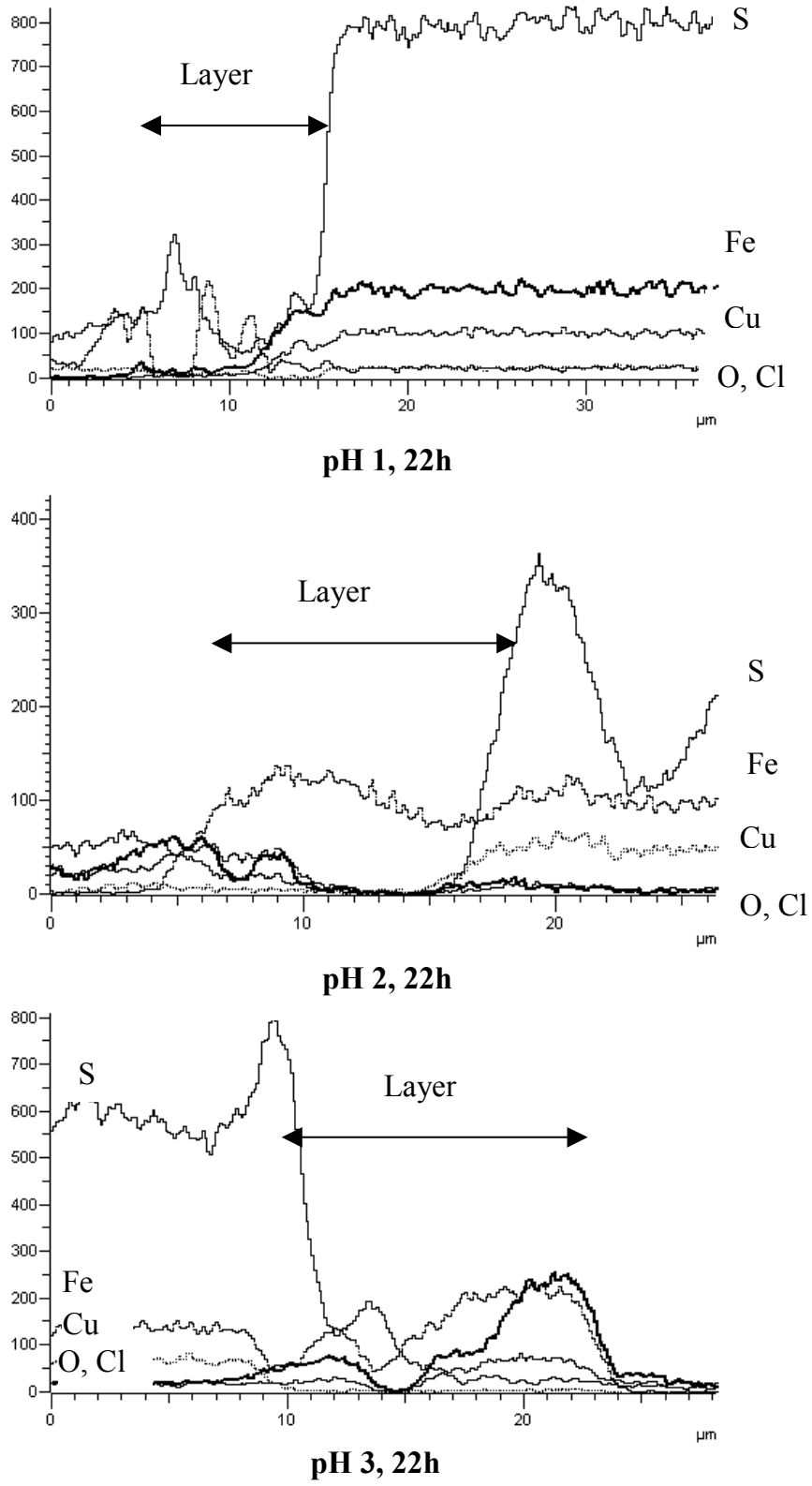

***Figure 9**. Line scan of the polished $CuFeS_2$ samples, leached at pHs 1 – 3 for 22 hours, where [NaCl] = 280 g/l, $[Cu^{2+}]$ = 30 g/l and T = 90 ºC. The curves on the base materials side from top to bottom are S, Fe, Cu, O and Cl. The side of the chalcopyrite base material varies: on the right at pHs 1 and 2, and on the left at pH 3.*

It was observed that the reaction product layer at pH 1 gave pulses for sulfur and grew from a thickness of ca. 1 μm to ca. 9 μm. At pH 2, for times t = 1 – 2 hours, the sulfur together with iron-oxygen (FeOOH) pulses (t = 4 – 22 h) were suggested, the thickness increasing from ca. 1 μm to ca. 10 μm. At pH 3, there were indications for both oxygen and iron (FeOOH) for all times measured and the layer thickness increased from ca. 1 μm to ca. 14 μm. The reaction product layer thicknesses are presented in Table 1, article [III] and Figure 10, article [III]. At all pHs the chalcopyrite reaction product layer thickness after 22 hours of leaching (9 – 14 μm) was 5 to 8 times higher than the layer thickness of 1.7 μm, reported by Parker et al. [65] in 0.1 M HCl solution after 22 hours of leaching at the OCP.

Line scans agreed with the earlier SEM study for polarized chalcopyrite electrodes (*Figure 8*). At pH 1, only sulfur pulses were observed at the reaction product layer, but no iron or oxygen. This suggests the presence of S^0 (*Figure 9*, pH1). At pH 2, sulfur pulses were observed at the early leaching hours (≤2 h), but also iron and oxygen pulses for leaching times longer than 2 hours (*Figure 9*, pH 2). At pH 3, strong oxygen and iron peaks were observed in the reaction product layer, and the presence of sulfur also became evident with increasing leaching time, t = 22 h. [III]

3.3 X-ray diffraction analyses

To confirm the phases present on the chalcopyrite surface, X-ray diffraction (XRD) analyses were carried out on the reaction product layers [V] formed on cubic (1 cm^3) chalcopyrite samples after 22 hours leaching at pHs 1 – 3 at the open circuit potential. After leaching, the samples were washed and dried and forwarded to Outotec Research in Pori for analysis. There the reaction product layer was separated from the mineral sample by careful scraping with a scalpel blade and the sample was analyzed by XRD. The results were published earlier in a table format [V]; Appendices 5 – 7 show the original XRD data. Appendix 5 shows that after 22 hours of leaching at pH 1, the reaction product layer consisted of elemental sulfur and a trace amount of goethite (analyzed as alpha $Fe_2O_3 \cdot H_2O$). At pH 2 (Appendix 6) the amount of FeOOH (ß-FeOOH, akaganeite) had increased, and S^0 was still present as suggested in article [III]. At pH 3 (Appendix 7), the reaction product layer consisted of FeOOH (akaganeite $Fe^{3+}O(OH)$, synthetic) and there were indications of S_8, where sulfur forms an eight-membered ring of sulfur atoms [57]. Also, the base mineral, chalcopyrite material, was detected in all XRD analyses.

With increasing pH, iron forms various iron oxide or iron oxide-hydroxide compounds. In this thesis, the XRD spectrum agreed with that of goethite (pH1), ß-FeOOH (pH2) and synthetic akaganeite (pH3). Due to the small number of XRD spectra, this thesis generally discusses FeOOH, as the iron product in the reaction product layer. This is intended to describe more of an iron compound, where iron is present as a trivalent species with two oxygen atoms and one hydrogen atom, than the exact phase structure. Earlier [59, 60], in ferric chloride media, FeOOH was found to occur in the form of ß-FeOOH, akaganeite.

3.4 Electrochemical Impedance Spectroscopy

When using electrochemical impedance spectroscopy (EIS), an appropriate electronic equivalent circuit, with components in series and parallel, can be fitted to the experimental data. A few EIS studies have been carried out on mineral surfaces, such as pyrite [68], chalcopyrite [69, 70], chalcocite (Cu_2S) [71] marmatite [72] and digenite $Cu_{1.87}S$ [73], but the author is unaware of any studies on chalcopyrite in cupric chloride solutions at elevated temperatures (90 °C). Those studies gave several interpretations and EIS equivalent circuits for sulfide mineral reaction product layers. Cabral et al. [68], Velásquez et al. [70] and Bevilaqua et al. [69] suggested a series layer model for both pyrite and chalcopyrite bioleaching and for chalcopyrite in borate solution. When writing the equivalent circuit in these systems, [] describes circuit elements in series and () in parallel. The circuit was of the form R(CR)(C[WR]), the first R representing the solution resistance, (CR) the surface layer and (C[WR]) the double layer and mass transport properties (*Figure 10 a*). Velásquez et al. [71], Shi et al. [72] and Nowak et al. [73] proposed a parallel layer model R(C[R(RC)]) for chalcocite in borate solution, marmatite-carbon paste electrodes in ferrous solutions and $Cu_{1.87}S$ in perchloric acid (*Figure 10 b*). This type of circuit is often used to represent an imperfectly covered electrode [71] or coated surfaces [74]. The equivalent circuit suggests that the bulk solution can attack the mineral both directly and through the reaction product layer.

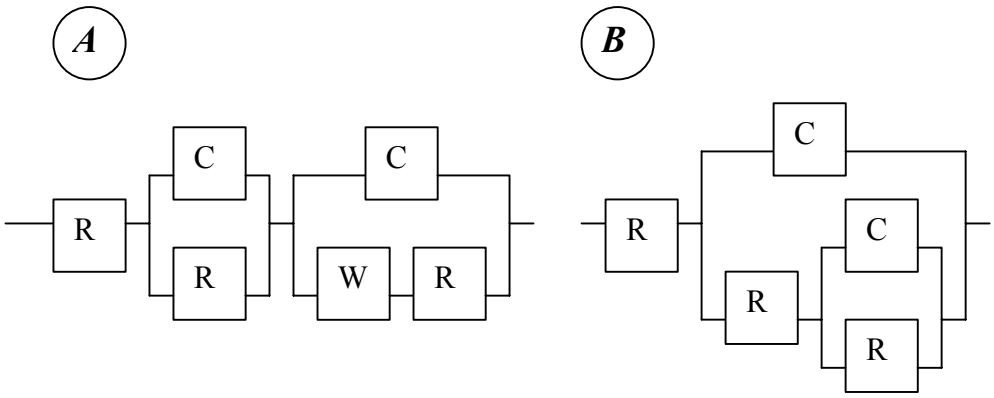

Figure 10. *Equivalent circuits having two time constants, (A) a series layer model R(CR)(C[WR]) and (B) a parallel layer model R(C[R(RC)]) on the left.*

Electrochemical impedance spectroscopy [V] was applied in order to complement the chalcopyrite leaching studies [I,III] with additional information about the electrochemical behavior of the chalcopyrite reaction product layers. The number of time constants present with increasing dissolution time (Table 2) and the total resistance values were estimated based on the EIS data. Equivalent circuits, published in [V], were fitted to the EIS data in order to determine the reaction product layer parameters. The low frequency loops were suggested to correspond the reaction product layer capacitances and resistances for solid-liquid reactions on chalcopyrite. However, the diffusion in a limited space leads frequently to a semicircle in the Nyquist plot. Therefore, the observed depressed semicircle at lower frequencies might also be associated with the diffusion through the layer of reaction products. The high frequency loop was suggested to reflect the apparent charge transfer resistance and the apparent capacitance of the chalcopyrite surface, but observed also to reflect the behavior of the reaction product layer. Therefore, it is reasonable to observe the total resistance,

polarization resistance ($R_1 + R_2 + R_3$), which can be seen at low frequencies in Nyquist plots [V] or Bode plots (*Figure 11* and *Figure 12*).

Table 2. The number of time constants present in the Nyquist plots at pHs 1, 2, and 3 as a function of time for a chalcopyrite electrode. The electrolyte composition was [NaCl] = 280 g/l, [Cu^{2+}] = 30 g/l, *T* = 90 °C. The arrow after the number describes, whether the total resistance (polarization resistance) of the system is increasing (↑) or decreasing (↓) after this time value.

	Time / hours						
pH	0.5	1	2	3	4	9	22
1	2 ↑	2 ↑	2 ↑	2 ↓	2 ↓	2 ↓	3
2	2 ↓	2 ↓	2 ↓	3 ↓	3 ↓	3 ↓	3
3	3 ↓	3 ↓	3 ↓	3 ↓	3 ↓	3 ↑	

It was concluded that the high frequency loop was a response mainly due to the capacitance of the chalcopyrite surface (apparent capacitance 0.1 – 100 μF/cm^2), whereas the low frequency loops reflected more the reaction product layer (apparent capacitance 1-100 mF/cm^2). The capacitance values also increased with increasing dissolution time at all pHs, which was explained by the chalcopyrite material reacting and forming more of the reaction product layer and so the surface area increased with time. Capacitances also increased with increasing pH, suggesting a more porous (greater surface area) reaction product layer at pH 3 compared to pH 1. Also, surface wetting may have increased the capacitance values.

It was shown that at pH 1 [V], for leaching times in the range 0.5 to 9 hours, there was generally a depressed semicircle at high frequency, followed by another incomplete semicircle at lower frequencies. The total resistance for reactions in the solid-solution interface in the system increased between 0.5 and 3 hours and then decreased. It was suggested that at pH 1, at first an elemental sulfur layer was formed on the chalcopyrite electrode surface. After 22 hours there was an indication of three time constants. The third time constant suggests the presence of a third phase, such as FeOOH, which was not detected in the earlier SEM/EDX measurements [III].

At pH 2, there were two semicircles during the first few hours, and a third time constant became evident at t = 3 h. The resistance for chemical reactions at the solid-solution interface decreased within the time scale studied. It is suggested that an elemental sulfur layer formed at the beginning of leaching. After approximately 3 hours, some FeOOH had formed (3rd time constant), which agrees well with the earlier SEM study [III]. The resistance for reactions on this elemental sulfur + FeOOH layer decreased with time. At 22 h the response of the electrode at pH 2 was very close to that at pH 1 after the same leaching time. Both reaction product layers at pH 1 and 2 had low resistance for reactions at the solid-solution surface at 22 hours and the OCPs were similar [V].

At pH 3, curves were obtained indicating three semicircles in the time range 0.5 – 9 h. Specifically, the third semicircle was incomplete. Three time constants suggested the presence of FeOOH, but also elemental sulfur, which could not be analyzed earlier [V]. The total resistance (polarization resistance) in the system decreased with time until 9 hours but increased after that. Between 3 and 9 h, the Nyquist plots at pHs 3 and 2 were similar, however, the difference after 22 h was remarkable: at pH 3, there was a semicircle followed by a long tail at an angle of 45° suggesting a Warburg-type diffusional component in the impedance (22 h). However, there is a possibility that this could also represent a time constant with a large mass transfer or charge transfer resistance. This behavior was found to be

reproducible. It suggested that after 22 h of leaching at pH 3 mass transport between solution and the chalcopyrite surface was limiting the chalcopyrite dissolution. [V]

The apparent charge transfer resistance was also observed to reflect partly the resistance of the reactions on the reaction product layer – solution interface. However, the total resistance (polarization resistance) of chalcopyrite was <80 Ωcm^2 for all simulated data sets. The bode plots shown in *Figure 11* and *Figure 12* show the total resistance of chalcopyrite as a function of pH. It can be seen that after 9 hours of leaching, the resistance was highest at pH 1. However, after 22 hours of leaching the resistance was highest at pH 3, being in the order of 150 Ωcm^2 (observed only from Bode plots, could not be simulated). This suggested that at longer leaching times (t = 22 h), the layer at pH 3 had the highest resistance for chemical reactions in the solid-solution interface. Another option is that diffusion in a limited space has caused this resistance. The resistance at pH 3 was still relatively low when compared with the studies of Velasquez et al. [70, 71] and Cabrera-Sierra et al. [75] (1×10^3 - 1×10^4 Ωcm^2) and cannot be stated as evidence of a passive layer. [V]

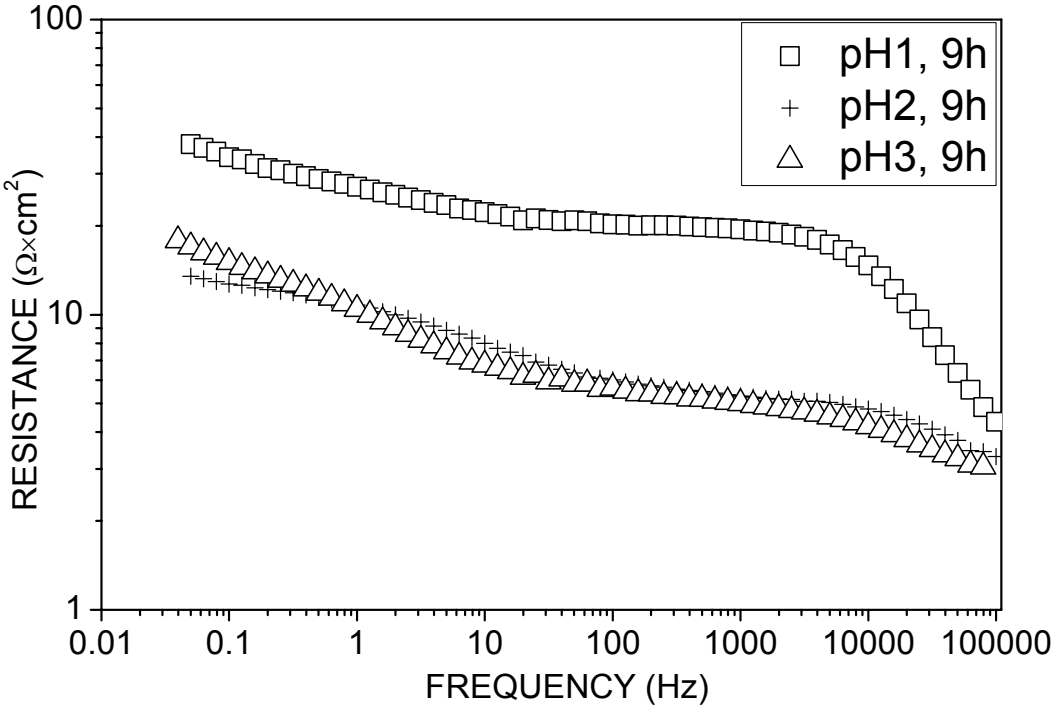

Figure 11. *Bode plot of EIS data after 9 hours of chalcopyrite leaching. [NaCl] = 280 g/l, [Cu^{2+}] = 30 g/l and T = 90 ºC.*

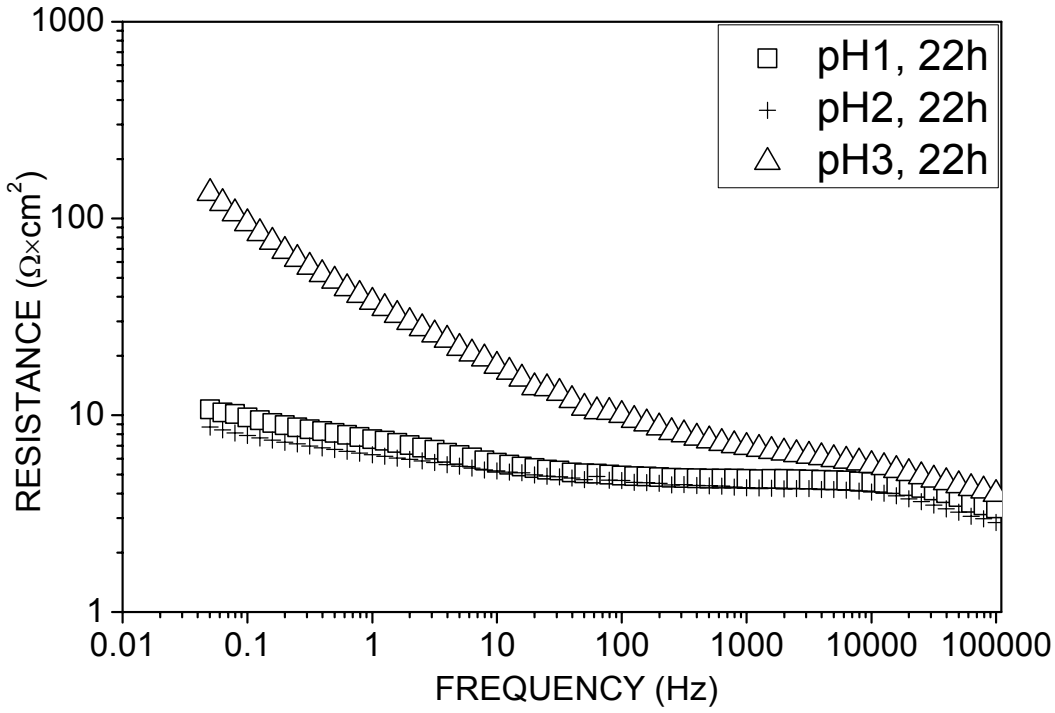

Figure 12. *Bode plot of EIS data after 22 hours of chalcopyrite leaching. [NaCl] = 280 g/l, [Cu^{2+}] = 30 g/l and T = 90 ºC.*

3.5 Reaction mechanism

It seems clear that the reaction occurring on a stationary chalcopyrite surface in a cupric chloride solution is the well-known oxidation reaction of chalcopyrite, producing cuprous ions, ferrous ions and elemental sulfur (1). Reaction (1) may also occur in sequence via dissolved H_2S species [64] resulting in the same net reaction. However, no evidence of H_2S formation was found, but any dissolved H_2S would be immediately oxidized to sulfur or copper sulfide by the excess of cupric ions. In this study, no partial dissolution products of chalcopyrite or precipitated secondary copper sulfides, such as covellite or chalcocite, were observed.

3.5.1 Reaction equilibrium

In cupric chloride solution, cupric ions can also oxidize ferrous ions (or chloro-complexes), forming cuprous and ferric ions or chloro-complexes (6). The Gibbs energy for this reaction is negative and the redox potential for cupric/cuprous is higher than for ferric/ferrous in concentrated cupric chloride solution (HSC 6.11). Ferric ions again can precipitate as FeOOH (7).

$$Fe^{2+}_{(aq)} + Cu^{2+}_{(aq)} \rightarrow Fe^{3+}_{(aq)} + Cu^{+}_{(aq)} \quad (6)$$

$$Fe^{3+}_{(aq)} + 2H_2O_{(l)} \rightarrow FeOOH_{(s)} + 3H^{+}_{(aq)} \quad (7)$$

Le Chatelier´s Principle states that a change in the concentration of a species shifts the equilibrium to the side, which reduces the change in concentration. It can be seen that decreasing acidity (increasing the pH) pushes reaction equilibrium (7) to the right. This causes reaction (6) to shift to the right as the amount of ferric in solution is decreased. This in turn shifts the equilibrium of $CuFeS_2$ reaction (1) to right. Reactions (1), (6) and (7) are rewritten below to represent the equilibrium of the total reaction more accurately.

$$CuFeS_{2(s)} + 3Cu^{2+}_{(aq)} \rightarrow 4Cu^{+}_{(aq)} + Fe^{2+}_{(aq)} + 2S^{0}_{(s)}$$
$$\downarrow$$
$$Fe^{2+}_{(aq)} + Cu^{2+}_{(aq)} \rightarrow Cu^{+}_{(aq)} + Fe^{3+}_{(aq)}$$
$$\downarrow$$
$$Fe^{3+}_{(aq)} + 2H_2O_{(l)} \rightarrow FeOOH_{(s)} + 3H^{+}_{(aq)}$$

3.5.2 Reaction kinetics

In this study it was observed that the resistance for chemical reactions occurring at the solid-solution interface was generally higher at pH 1 than at pH 3 (V). This was valid especially with short leaching times. This behavior suggests that at pH 3, the precipitation of FeOOH increases the chemical reaction rate (1,6,7), whereas at pH 1 these reactions are all slower.

Figure 13 characterizes roughly the mechanism of chalcopyrite electrode dissolution in cupric chloride solutions. At pH 1, during the first few minutes, chalcopyrite dissolution is fast (III,V) and it is likely that reaction (1) occurs, *Figure 13* a. However, the gray elemental sulfur (S^0) remains at the chalcopyrite surface and the resistance for chemical reactions increases almost immediately (V), *Figure 13 b*. This layer is porous and easily removable, but it may decrease the chemical dissolution reaction rate by increasing the concentration of Cu^+

(cuprous chloro complex) and Fe^{2+}/Fe^{3+} on the mineral surface. Based on the potentiostatic experiments (III, V), the elemental sulfur-rich reaction product layer at pH 1 presents a greater barrier to dissolution than the FeOOH layer at pH 3. The kinetics of FeOOH formation at pH 1 is very slow. The slow dissolution kinetics at pH 1 can also be due to the formation of a metal-deficient phase on chalcopyrite surface, which makes the surface nobler [65,84,85]. With increasing time, FeOOH will also form in the reaction product layer at pH 1 (V) decreasing the resistance for chemical reactions on the chalcopyrite surface, *Figure 13 c*. The slow chemical reaction rate does not favor chalcopyrite dissolution at pH 1.

At pH 3, the dissolution reaction (1) also occurs during the first few minutes, *Figure 13 d*. Both elemental sulfur and FeOOH start to form on the chalcopyrite surface, since the ferrous species formed react with the excess concentration of cupric ions (6). It seems evident that both elemental sulfur and FeOOH stay on the surface [V], Table 2 and *Figure 13 e*. Chalcopyrite dissolution behind this layer is faster than at pH 1 and the reaction product layer is thicker [III], *Figure 13 f*. FeOOH formation beside the elemental sulfur favors chalcopyrite dissolution by (i) decreasing the resistance [V] for chemical reactions (1), (6) and (7) and by (ii) making the reaction product layer less hindering for diffusion of solution species [III, V].

At pHs between 1 and 3, the chalcopyrite dissolution is a combination of these two dissolution mechanisms (*Figure 13*) as shown by the color of the surface (*Figure 7*), SEM line scans (*Figure 9*) and EIS data (Table 2), [V]. It can be concluded that by increasing the pH from 1 to 3, the precipitation kinetics of FeOOH increases and chalcopyrite dissolution becomes more favorable. With increasing time, FeOOH can be seen already at lower pHs, this favors chalcopyrite dissolution as well.

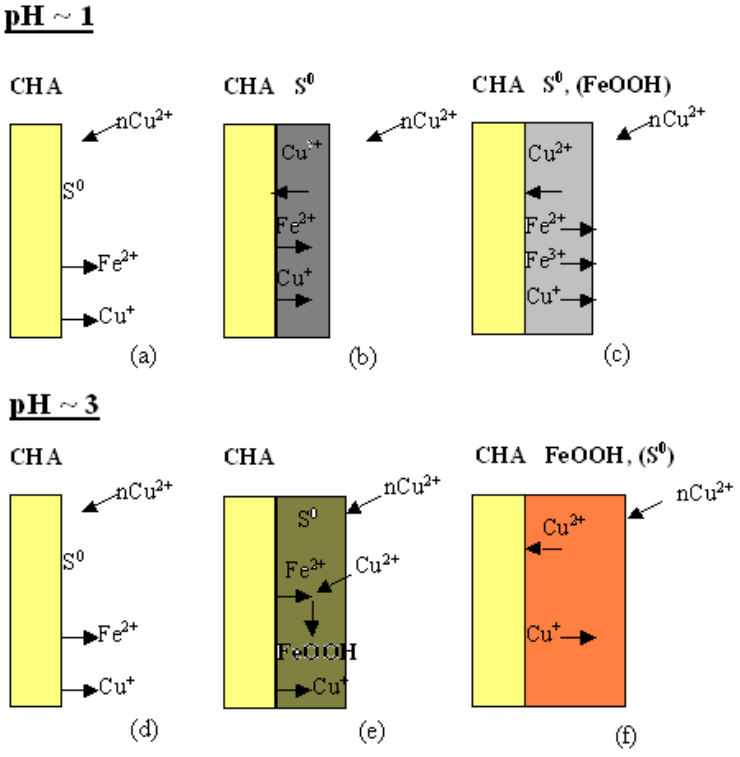

Figure 13. *Characterized mechanism of chalcopyrite (CHA) electrode leaching at pH 1 (a – c) and at pH 3(d – f) in cupric chloride solutions. Cl^- ions are not illustrated. Cu^{2+}, Cu^+, Fe^{3+} and Fe^{2+} are used to describe the general oxidation state of metal ions and not the exact form of the species, since metal ions readily form chloro-complexes in concentrated chloride solution.*

4 RATE CONTROLLING STEP

In chalcopyrite leaching, the rate-controlling step can be related to diffusion processes or chemical reactions. The overall reaction rate can be controlled by:

(1) Diffusion of a reactant from the bulk solution to the chalcopyrite surface
(2) Diffusion of a reactant or a reaction product through the reaction product layer
(3) Anodic dissolution reaction rate on the chalcopyrite surface or
(4) Cathodic reduction reaction on the chalcopyrite or reaction product surface.

4.1 Activation energy

It has been suggested that an activation energy (E_a) of greater than 40 kJ/mol indicates that the reaction is controlled by charge transfer (chemical or surface-controlled processes). Low E_a values (<20 kJ/mol) have been suggested to relate to diffusion-controlled processes [76].

The activation energy for chalcopyrite dissolution in ferric chloride solution has been widely studied and the activation energies determined have been listed several times [15, 29, 61, 66, 77]. The synergistic effect of cupric chloride in ferric chloride systems has also been observed [15, 29]. The solutions, temperatures, concentrations, and mineral sources in the studies vary, but generally the activation energy values in ferric chloride solutions have been in the range of 40 to 80 kJ/mol, i.e. chemical control [15, 29, 61, 66, 77]. E_a is almost independent of the geographical origin of the chalcopyrite sample as well [78]. The E_a values for chalcopyrite in chloride media have been related to the chemical or surface controlled processes, controlled by charge transfer. Exceptionally, Havlik et al. [62] suggested a two-mechanism leaching process for chalcopyrite in ferric chloride solution. At higher temperatures, a chemical control (E_a = 68.9 kJ/mol) was suggested, whereas in the temperature range 3.5 – 45 ºC, a diffusion-controlled leaching process (E_a = 1.1 kJ/mol), accompanied by the formation of intermediate sulfides was proposed. In contrast, Godocikova et al. [79] suggested that the dissolution mechanism of very impure chalcopyrite in ferric chloride solutions at 50 - 70 ºC is under mixed control, whereas at higher temperatures (70 – 90 ºC) it is controlled by diffusion.

Few activation energies for chalcopyrite leaching in cupric chloride solutions are available in literature. An activation energy of 134.7 kJ/mol [13] was reported for chalcopyrite in cupric chloride solution ($[Cu^{2+}]$ = 0.79 M, $[Cl^-]$ = 6.23 M, T = 50 – 97.5 ºC). The rate-controlling step was suggested to be a step in the anodic reaction. Wilson et al. could not, however, explain the meaning of such a large value for the activation energy. Hirato et al. [16] reported an activation energy of 81.5 kJ/mol ($[Cu^{2+}]$ = 0.1 M, [HCl] = 0.2 M, T = 60 – 90 ºC) and Bonan et al. [17] reported activation energy of 71 kJ/mol (17 kcal/mol) with $[Cu^{2+}/Cu^+]$ = 1, [NaCl] = 4.0 M, T = 85 – 103.9 ºC. Even higher values were suggested at lower temperatures [17]. All these values suggest that chemical or surface processes control the dissolution of chalcopyrite in cupric chloride solution.

In this thesis, the activation energy of the reaction at pH 2 was estimated using the Arrhenius equation [I]. The current densities were taken from the anodic polarization curves in a pH 2 solution [50] at T = 70 – 90 ˚C, at potentials 0.8, 0.9 and 1.0 V vs. SHE (0.6, 0.7 and 0.8 V vs.

Ag/AgCl). By plotting log(k) vs. 1/T with each Cu^{2+} concentration (0.9 – 26.6 g/l), a plot where the slope was -E_a/R·2.303 was obtained. From *Figure 14* it can be seen that the dependence of E_a on the cupric ion concentration was not clear. However, it was seen that generally at 0.8 V vs. SHE (0.6 V vs. Ag/AgCl), E_a was <45 kJ/mol. At 0.9 V vs. SHE, E_a was <35 kJ/mol and at 1.0 V vs. SHE, E_a was <25 kJ/mol, but all > 18 KJ/mol, which is indicative of mass diffusion control.

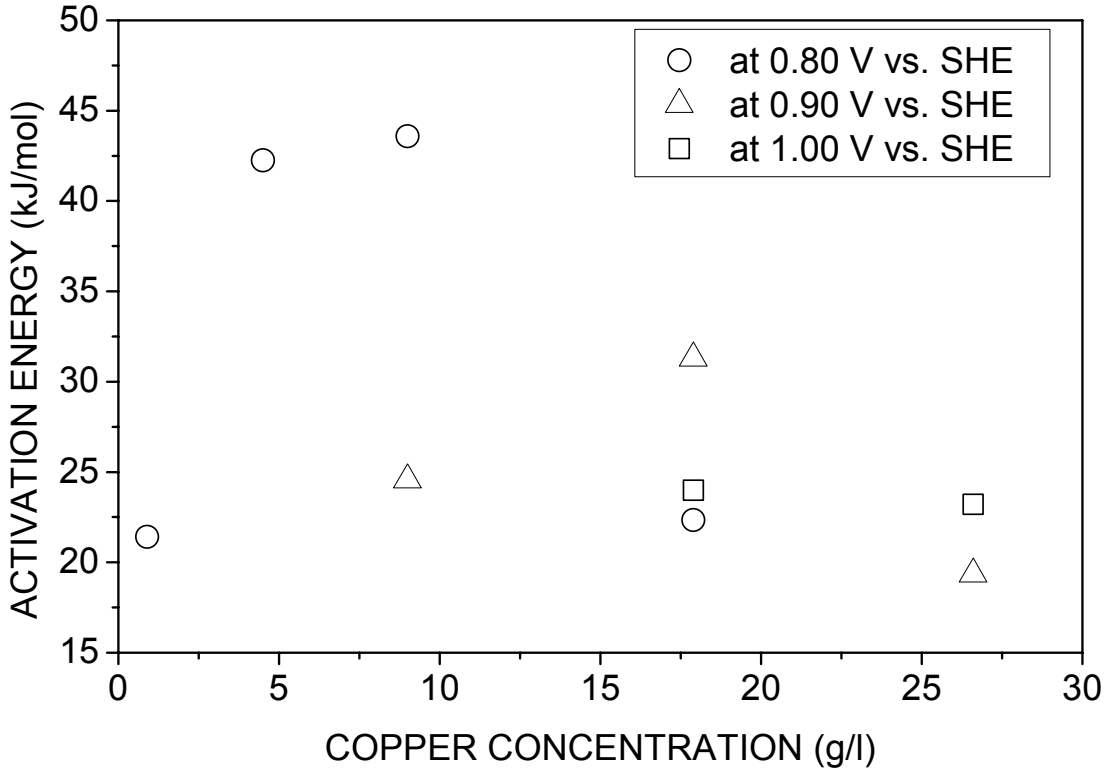

Figure 14. *Activation energies (E_a) as a function of cupric ion concentration. The E_a values have been calculated at E = 0.80, 0.90 and 1.00 V vs. SHE (0.60, 0.70 and 0.80 V vs. Ag/AgCl), T = 70 – 90 ˚C. Where [NaCl] = 250 g/l and pH = 2.*

4.2 Exchange current density, diffusion coefficient and charge transfer resistance

An estimation of the exchange current density (j_0) was obtained by the Tafel method [II], using data from the cathodic polarization curves obtained with a platinum working electrode. The exchange current density can depend on the electrode material. *Figure 15* shows, however, that the cathodic reactions on platinum are similar to those on chalcopyrite, and platinum can be used to study the cathodic reactions. The exchange current density was independent of cupric ion concentration in the range $[Cu^{2+}]$ = 10 – 40 g/l and gave an average value of j_0 = 4.6 mA/cm^2, corresponding to an electron transfer rate constant (k^0) value of 1.5×10^{-4} cm/s. It is clear that the j_0 value for the cathodic reaction (4.6 mA/cm^2) was larger than that of the anodic reaction (<1.2 mA/cm^2, [I]). Thus, it can be suggested that the cathodic reaction rate did not limit the rate of chalcopyrite dissolution.

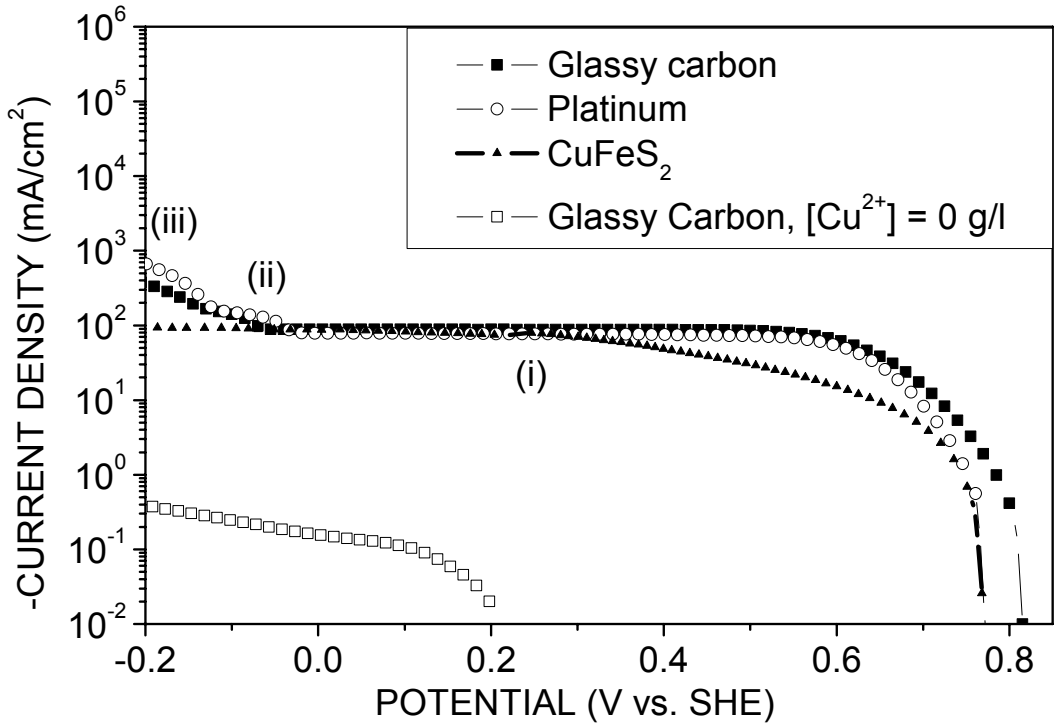

Figure 15. *Cathodic polarization curves for glassy carbon, platinum and chalcopyrite RDEs (100 rpm). [NaCl] = 280 g/l, [Cu^{2+}] = 20 g/l (for three upper curves) and [Cu^{2+}] = 0 g/l (for the lowest curve), sweep rate = 0.7 mV/s, pH = 2 and T = 90 °C.*

The diffusion coefficient of Cu^{2+} or the cupric-chloro complex in the bulk cupric chloride solution (pH 2) was calculated to be $8.3\pm0.3\times10^{-6}$ cm^2/s at E = 0.197 V vs. SHE (E = 0 V vs. Ag/AgCl) [II]. This is of the same magnitude as the values published for cupric and cuprous species in chloride media, D ($[CuCl]^+/CuCl_2$) = 5.3×10^{-6} cm^2/s and D ($[CuCl_2]^-/[CuCl_3]^{2-}$) = 7.3×10^{-6} cm^2/s [80, 81]. In this study, the diffusion coefficient of Cu^{2+} or the chloro-complex in the reaction product layer formed at E = 0.9 – 1.1 V vs. SHE was calculated to be 1.4×10^{-9} cm^2/s at pH 2 [I]. This may also be an effect of the current representing the reaction occurring only on a small part of the chalcopyrite surface, which was not covered by the reaction products. Although one cannot confirm the diffusion coefficients at the OCP, it is unlikely that the diffusion of cupric ions or complexes in the solution is the rate-limiting step in chalcopyrite dissolution. In contrast, the diffusion coefficient calculated at anodic potentials was relatively low as the reaction product layer covered the reactive chalcopyrite surface.

4.3 Rate controlling step as a function of pH

The apparent charge transfer resistance and the resistance at the reaction product layer – solution interface were calculated using an equivalent electrical circuit to fit the EIS data [V]. When comparing the apparent charge transfer resistances and reaction product layer resistances to the dissolution rates of chalcopyrite in the potentiostatic curves, it can be concluded that the high total polarization resistances at pH 1 in the early stages of the measurement were in good agreement with the low dissolution rates in the potentiostatic curves [III][V]. However, decreasing total polarization resistances during the first hours at pH

2 and 3 did not show any corresponding increase in the dissolution rates in the potentiostatic curves. This suggests that at pH 1, the anodic reaction rate can have limited the dissolution, but not at pH 2 or 3. In addition, the activation energy values calculated suggested that at pH 2 the dissolution is more diffusion controlled.

In the potentiostatic experiments [III], it was shown that the chalcopyrite dissolution rate was fast at the beginning of leaching in cupric chloride solution. The dissolution rate decreased strongly within the first 500 seconds. After that the current, or dissolution rate, stayed constant or decreased slightly. This demonstrates that chalcopyrite dissolution was fast in the first minutes of leaching and then decreased with time. The potentiostatic data here is presented as a function of time square root (*Figure 16*). The leaching kinetics was shown to be parabolic at pH 3, changing more into inverse parabolic at low pHs. This supports the claim that diffusion through the reaction product layer limits dissolution at pH 3, where as at pH 1 the chemical reaction rate might also limit chalcopyrite dissolution.

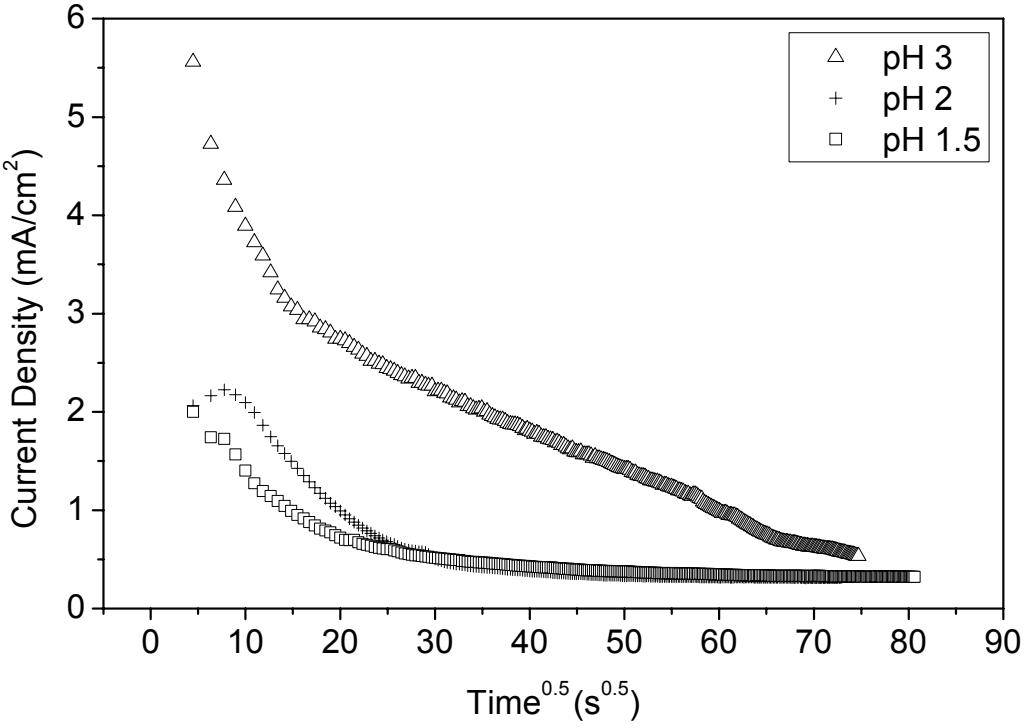

Figure 16. *Current density as a function of time square root at 650 mV vs. Ag/AgCl. [NaCl] = 250 g/l, [Cu^{2+}] = 17.9 g/l T = 85 °C.*

5 SPECIES IN CUPRIC CHLORIDE SOLUTIONS

The standard electrode potentials, E^o, for copper ions and copper, calculated with the HSC 6.1 thermodynamic calculation software at 25 ° C were as follows (8) – (10):

$$Cu^{2+}_{(aq)} + 2e^- = Cu_{(s)} \qquad E^o = 0.337 \text{ V vs. SHE} \qquad (8)$$

$$Cu^{2+}_{(aq)} + e^- = Cu^{+}_{(aq)} \qquad E^o = 0.156 \text{ V vs. SHE} \qquad (9)$$

$$Cu^{+}_{(aq)} + e^- = Cu_{(s)} \qquad E^o = 0.518 \text{ V vs. SHE} \qquad (10)$$

The standard electrode potentials for the copper species suggest that in an aqueous solution it is more likely that Cu^{2+} would reduce straight to metallic copper, instead of going first to the cuprous intermediate Cu^+. However, these thermodynamic values cannot be applied to concentrated chloride solutions, due to the complex formation and incomplete information about the activity coefficients in concentrated alkali metal chloride solutions.

The advantage and one very strong characteristic feature of a chloride solution is that it can form complexes with copper cations and thus stabilize cuprous ions as various cuprous complexes, i.e. cuprous chloro-complexes stabilize the product of the reduction reaction. Thus, for example, reduction reactions, such as (13) – (18) can be possible in strong alkali metal chloride solutions.

5.1 Cathodic reactions

In the HydroCopper® process, cupric ions in chloride solutions are used as an oxidant to leach sulfide minerals such as chalcopyrite. In article [II] the kinetics of cupric ion or cupric chloro-complex reduction in concentrated cupric chloride solutions were studied. The reacting species in the solution were not known precisely. When leaching chalcopyrite there occur both anodic dissolution reaction and cathodic cupric ion or chloro-complex reduction reactions. Then the rates of anodic and cathodic reactions are equal. The reduction reaction cannot be studied using chalcopyrite, which makes it necessary to study the cathodic reactions of cupric chloride solutions using inert electrode such as platinum (*Figure 15*).

The anodic reaction is the oxidation of sulfur from the chalcopyrite lattice, whereas the cathodic reaction is the reduction of cupric ions or copper(II) complexes to cuprous. Cathodic reactions in concentrated cupric chloride solutions were presented in article [II]. The reactions possible were suggested to be (i) the reduction of $[CuCl]^+$ to the complex $[CuCl_3]^{2-}$, (ii) the reduction of $[CuCl_3]^{2-}$ to solid copper at $E \approx$ -0.05 V vs. SHE (-0.25 V vs. Ag/AgCl) and (iii) hydrogen evolution. The copper species were based on the literature referenced in the paper. The complexation of cupric ions is discussed later in section 5.3.

From the cathodic polarization curves, the diffusion coefficient for $[CuCl]^+$ calculated by the Levich method [53] was 8.3±0.3 $\times 10^{-6}$ cm^2/s and the corrected value obtained with the Gregory-Riddiford method [82] was 8.8±0.4 $\times 10^{-6}$ cm^2/s. The unit rate constant, k_T, was concluded to be independent of the cupric ion concentration, but dependent on the RDE rotation rate. The average unit rate constants are in the range 2.0–10.1 $\times 10^{-3}$ cm/s for rotation rates in the range 100 to 2500 rpm. [II]

5.2 Cuprous complexation

In a literature survey of the main cuprous complexes published by the author [42, 50, 51] the predominant cuprous complex was generally identified as $[CuCl]^0$ at low (<0.1 M) chloride concentrations. At higher chloride concentrations (>0.1 M), the stabilities of cuprous complexes $[CuCl_2]^-$, $[CuCl_3]^{2-}$ and $[CuCl_4]^{3-}$ increased.

It is widely suggested that in chloride solutions Cu^+ readily forms stable chloro-complexes with up to four chlorides, such as $[CuCl]^0$, $[CuCl_2]^-$, $[CuCl_3]^{2-}$, $[CuCl_4]^{3-}$ and that Cu^+ in the complex form is very stable. In article [IV] the complexation of cuprous copper was studied unconventionally using redox potential measurements as an experimental method. The redox potentials of several copper chloride solutions were measured for 50 days. All copper was originally added as cupric chloride. The redox potential was plotted against temperature. According to the Nernst equation, the slope in this kind of curve is equal to $R/zF \times \ln(Cu^{2+}/Cu^+)$ and E^o can be determined from the y-axis intercept, with T = 0 K. The standard electrode potential determined mathematically from the experimental redox potentials was E^o = 0.158 (±0.121) V vs. SHE in the HydroCopper® solution. It was assumed that the (Cu^{2+}/Cu^+) ratio is constant at all cupric concentrations and the redox potential was affected only by temperature. After 49 days, the cuprous concentrations were very low (in the order of 10^{-15} mol/m^3) but the cupric concentrations stayed at the original level (1.6×10^{-4} – 6.3×10^{-4} mol/m^3). This was predictable, since the solution was stored in a closed bottle and nothing was added during the storing time. These concentrations of cuprous and cupric species were calculated using Nernst equation and the E^o value defined experimentally.

With HSC 6.1 software, the following standard electrode potentials were calculated at T = 25 °C (298 K) for cupric and cuprous species (11) – (18). The cupric species are presented in the equations on the left and cuprous on the right. In equations (11) – (12), cuprous is not in a chloro-complex form, where as in the equations (13) – (18) cuprous is in a chloro-complex form of $[CuCl]^0$, $[CuCl_2]^-$ or $[CuCl_3]^{2-}$. At low concentrations it has been suggested that $[CuCl]^0$ is the prevailing species [37, 83], reactions (15) and (18). Cupric was assumed not to be complexed (13) – (15) (section 5.3), but also values for Cu^{2+} in a chloro-complex form $[CuCl]^+$ are presented (16) – (18).

$$Cu^{2+}_{(aq)} + e^- = Cu^+_{(aq)} \qquad E^o = 0.156 \text{ V vs. SHE} \qquad (11)$$

$$[CuCl]^+_{(aq)} + e^- = Cu^+_{(aq)} + Cl^-_{(aq)} \qquad E^o = 0.133 \text{ V vs. SHE} \qquad (12)$$

$$Cu^{2+}_{(aq)} + 3Cl^-_{(aq)} + e^- = [CuCl_3]^{2-}_{(aq)} \qquad E^o = 0.494 \text{ V vs. SHE} \qquad (13)$$

$$Cu^{2+} + 2Cl^-_{(aq)} + e^- = [CuCl]_2^-{}_{(aq)} \qquad E^o = 0.470 \text{ V vs. SHE} \qquad (14)$$

$$Cu^{2+} + Cl^-_{(aq)} + e^- = [CuCl]^0_{(aq)} \qquad E^o = 0.558 \text{ V vs. SHE} \qquad (15)$$

$$[CuCl]^+_{(aq)} + 2Cl^-_{(aq)} + e^- = [CuCl_3]^{2-}_{(aq)} \qquad E^o = 0.454 \text{ V vs. SHE} \qquad (16)$$

$$[CuCl]^+ + Cl^-_{(aq)} + e^- = [CuCl]_2^-{}_{(aq)} \qquad E^o = 0.447 \text{ V vs. SHE} \qquad (17)$$

$$[CuCl]^+_{(aq)} + e^- = [CuCl]^0_{(aq)} \qquad E^o = 0.535 \text{ V vs. SHE} \qquad (18)$$

The E^o for the redox pairs with a cuprous ion in a chloro-complex form (13) – (18) is at least 0.3 V higher than E^o for the redox pairs where cuprous is not complexed with chloride (11)-(12). It was shown that the experimentally determined E^o values were almost independent of the cupric ion concentration [IV], as stated by the Nernst equation. In contrast, some variation of the redox potential with time was seen. Even with the large margin of error (E^o = 0.158 (±0.121) V vs. SHE), high potentials typical for redox couples having cuprous in a chloro-complex form (13) – (18), cannot be reached. This suggests that in highly concentrated cupric chloride solutions, cuprous is mainly present as uncomplexed Cu^+ ions, at very low cuprous concentrations (in the order of 10^{-15} mol/m^3). The reduction of cupric to cuprous species occurred faster (in 5 days) in a more concentrated solution, having a total concentration of copper species of 40 g/l. Solutions which originally had 30, 20 and 10 g/l reached the steady state within 20, 26 and 26 days, respectively.

Earlier at much higher Cu^+ concentrations, cuprous ions have constantly been suggested to be in the form of complexes [30, 32-41]. The presence of uncomplexed cuprous ions in concentrated chloride solutions, with very low cuprous concentrations is a novel finding in the field of chloride chemistry. In future, possibly UV-visible spectroscopic methods could be used to study this phenomenon more closely, as uncomplexed and complexed species have individual characteristic absorption peaks [25].

5.3 Cupric complexation

The complexation of cupric ions in concentrated chloride media is still a matter for debate. Berger *et al.* [30] reported in their review article that at low Cl^- concentrations the hexa-aqua copper complex $[Cu(H_2O)_6]^{2+}$ is the dominant species and in more concentrated solutions $[CuCl]^+$ and $[CuCl_2]^0$ dominate. As the chloride concentration reaches 2.5 M, $[CuCl_3]^-$ is formed and with 5 to 10 M of chloride $[CuCl_4]^{2-}$ is the main species. Collins et al. [33] concluded that no complexation between Cu^{2+} and Cl^- occurs below a temperature of 75 °C with 0.2 and 2.2 M Cl^-. With higher chloride concentrations, however, e.g. [NaCl] = 5 M, $[CuCl]^+$ was observed to be the dominant species at 25-75 °C, becoming $[CuCl_3]^-$ and $[CuCl_4]^{2-}$ at 125 °C. Generally Collins [33] summarized that the stability of the $[CuCl]^+$ complex appears to be overestimated. Christov also [32] assumed that Cu^{2+} does not form any chloride complexes.

In an earlier publication [42], redox potentials in cupric chloride solutions were calculated using HSC 5.11 thermodynamic software. The redox potentials were taken from E-pH diagrams, which were calculated at 90 °C with $[Cu^{2+}]$ = 0.41 M and $[Cl^-]$ = 5.1. The redox potential of $Cu^{2+}/[CuCl_3]^{2-}$ (13) was calculated to be ca. 0.65 V vs. SHE, whereas the redox potential of $[CuCl]^+/[CuCl_3]^{2-}$ (16) was lower at ca. 0.55 V vs. SHE. This shows that the redox potential of concentrated cupric chloride solutions can be higher if Cu^{2+} does not form chloro-complexes. Experimentally, the redox potential was measured to be 0.76 – 0.95 V vs. SHE (0.56 – 0.75 V vs. Ag/AgCl) [IV]. The experimentally measured redox potential was observed to be closer to the thermodynamically calculated redox potential, when Cu^{2+} was not complexed with chloride ions. This behavior was also characteristic for other redox couples; generally the standard electrode potentials with Cu^{2+} as an ion (hexa-aqua copper) (13) – (15) were higher than those having a cupric ion in a chloro-complex form (16) – (18).

Recently, Pihlasalo et al. [43] validated a new MTAQ (vers. 3.2) aqueous database for concentrated chloride solutions which used a modified Pitzer model for aqueous solutions, similar to those used in the HydroCopper® process. The model reproduced well the excess Gibbs energy of an aqueous solution phase over a wide range of temperatures and concentrations. Their calculations show that in the first leaching stage of HydroCopper® ([NaCl] = 4.28 mol/kg, [CuCl] = 0.95 mol/kg, $[CuCl_2]$ = 0.16 mol/kg and $[Na_2SO_4]$ = 0.11 mol/kg) at low chalcopyrite concentrations, the prevailing cupric species is the hexa-aqua cupric ion and not a cupric chloro-complex (*Figure 17*). In the same environment the prevailing Cu^+ species is $[CuCl_3]^{2-}$.

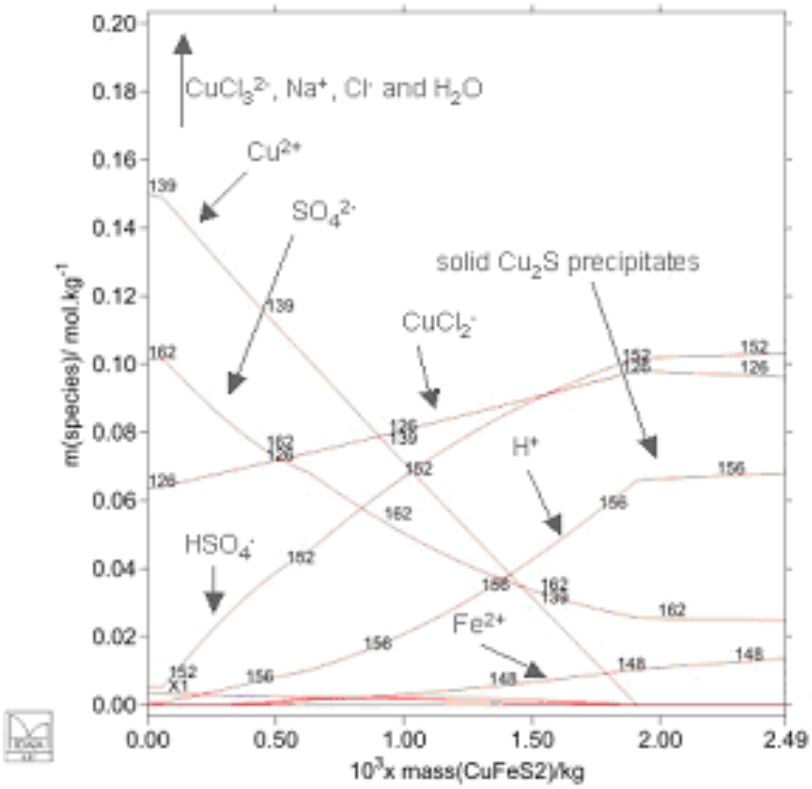

Figure 17. *The prevailing species in the first leaching stage of HydroCopper® process as a function of increasing chalcopyrite concentrate amount ([NaCl] = 4.28 mol/kg, [CuCl] = 0.95 mol/kg, [$CuCl_2$] = 0.16 mol/kg and [Na_2SO_4] = 0.11 mol/kg). Validation of the MTAQ aqueous database with HydroCopper® process data. NB, the X-axis is the mass of $CuFeS_2$ in kilograms. [43]*

Based on the redox potential measurements [IV], HSC 5.11/6.1 database and a literature survey [I, II] it was suggested that in concentrated cupric chloride solutions, the cupric ion can stay at least partially not chloro-complexed. The novel calculations using the MTAQ database [43] confirmed that the prevailing cupric species in concentrated chloride solution is the cupric ion and not a cupric chloro-complex.

6 DISCUSSION

This study was based on three scientifically interesting hypotheses about chalcopyrite reaction product layers, the rate-limiting step in chalcopyrite leaching and solution species in cupric chloride solutions. Electrochemical techniques, such as anodic and cathodic polarization, potentiostatic experiments, redox measurements and electrochemical impedance spectroscopy were applied both with stationary and rotating disk chalcopyrite electrodes. Complementary microscopy methods, such as stereo-optical microscopy and scanning electron microscopy as well as X-ray diffraction were also used. Thermodynamic software HSC 5.11 and 6.1 was applied for reduction-oxidation couple observations. These methods resulted in a wide set of data about the formation of the reaction product layers on chalcopyrite with time, the phases present, the resistances and capacitances for reactions on the chalcopyrite and reaction product layer, the rate limiting step for chalcopyrite dissolution, and how all of these change with respect to pH. Additionally, a set of redox potential values as well as E^o value was determined. The experiments were mainly carried out at high solution temperatures ($T \geq 90$ ºC), representative of the industrial case, HydroCopper®.

During the leaching of chalcopyrite the anodic reaction is the oxidation of sulfur in the mineral lattice. The cathodic reaction is the reduction of cupric ions or complexes. Oxidation of sulfur in the mineral releases metal ions into the solution. This can also result in a new metal-deficient phase [65,84,85] on the mineral surface, which can be nobler than the original mineral itself. As the dissolution of the mineral lattice continues, it will eventually break down leaving elemental sulfur. The elemental sulfur, metal-deficient layer, precipitated compounds, metal ions and metal chloro-complexes in the solution produce complex reaction product layers on a dissolving chalcopyrite surface. The composition, thickness, and permeability of the reaction product layer depend on the solution properties. The most important effect of the reaction product layer is that it hinders both the mass transfer of the cathodic reactant from the bulk solution to the mineral surface and diffusion of dissolved metals from mineral surface to the solution. The properties of the reaction product layer depend on the solution pH. At low pHs, the hydrated metal ions or complexes remain in solution and diffuse away from the chalcopyrite surface. This leaves only the metal-deficient layer and elemental sulfur to form the reaction product layer that effectively hinders dissolution. At high pHs, the metal ions can also form hydroxides or hydrated oxides. These compounds can precipitate out on the mineral surface, creating more permeable areas in the reaction product layers.

The composition of the chalcopyrite reaction product layer and formation of phases as a function of time and pH were studied. The product layer forming on a reacting chalcopyrite surface has been widely studied in sulfate solutions and ferric chloride solutions, but there were only a few studies in concentrated cupric chloride solutions. In a concentrated cupric chloride solution, at temperatures near to the boiling point of the solution, the reaction product layer on the surface of solid chalcopyrite was strongly affected by the pH of the solution.

At lower pHs, near to 1, a gray one-phase elemental sulfur layer formed at $t \leq 9$ h. With longer leaching times, a two-phase layer of elemental sulfur and FeOOH formed. The reaction product layer at pH 1 allowed a slower dissolution, than the reaction product layer at higher pH values. The resistance for reactions occurring at the solid - solution interface

increased until t = 3 h and then decreased. At pH 2, the layer was a one-phase elemental sulfur layer during the first few hours (t < 3 h), but the second phase, FeOOH, was observed already after 3 hours of leaching. The resistance for reactions at the solution - reaction product layer interface decreased with time up to 22 hours. At higher pH values, near to pH 3, a yellow-orange color iron-oxygen rich two-phase reaction product layer formed. Two phases were present at all times, up to 22 hours. The layer was analyzed to be mainly FeOOH, and elemental sulfur was also present. This layer allowed faster chalcopyrite dissolution in the first few hours. Also, the resistance for chemical reactions in the solid-solution interface was lower during the first few hours. The resistance for reactions on the chalcopyrite reaction product layer was low at all pHs and leaching times (<150 Ωcm^2), compared to literature values found for some other reaction product layers (1×10^3 - 1×10^4 Ωcm^2) [70, 71, 75].

It was shown that FeOOH formed in the reaction product layer in addition to the elemental sulfur by increasing the pH from 1 to 3 and with increasing time. This precipitation favored cupric ion or chloro-complex reduction by ferrous species, likely a chloro-complex, and thus also chalcopyrite dissolution. This was seen as a decrease in the resistance for chemical reactions (EIS). The dissolution at pH 1, having a metal-deficient layer and elemental sulfur, was slower than dissolution through the layer having a FeOOH rich layer at pH 3.

For chalcopyrite leaching, the rate-controlling step may be due to the anodic dissolution process, cathodic reduction process, diffusion in the solution or diffusion in the reaction product layer. The exchange current density estimated from the cathodic polarization curves (4.6 mA/cm^2) was higher than that estimated from the anodic polarization curves (<1.2 mA/cm^2). This suggested that the cathodic reaction was not the rate-controlling step. In EIS measurements, generally no Warburg tail was observed (with the exception of pH 3, 22 h), which suggested that diffusion in the solution was not the rate-controlling step. Activation energies calculated for chalcopyrite were 18 – 45 kJ/mol and suggested that the rate-controlling step at pH 2 was diffusion. Total polarization resistances calculated using EIS data compared to potentiostatic curves showed that at pH 2 or 3 it was not the chemical reaction in the chalcopyrite – solution or in the reaction product layer – solution interface that limited chalcopyrite dissolution. However, at pH 1, the chemical reaction rate may have limited dissolution. Potentiostatic curves confirmed parabolic kinetics at pH 3 suggesting diffusion-controlled leaching. This changed into inverse parabolic kinetics at pH 1, suggesting a chemical reaction controlled process. Thus it must be a diffusion in the reaction product layer that controls the rate of chalcopyrite dissolution at pH 3, changing into a more charge transfer controlled process at pH 1.

It was shown that the resistance at the reaction product layer – solution interface or apparent charge transfer resistance did not limit the leaching kinetics at higher pHs. Then the dissolution rate of the solid chalcopyrite species was controlled by diffusion through the reaction product layer. The reaction product layer was also shown to be porous and easily removable. In a real process, there are inter-particle collisions and abrasion occurring in the reaction vessels. The reaction product layers are affected strongly by the mechanical collisions and removed during the mixing continuously exposing a fresh surface for leaching. This suggests that the leaching parameters in a real process can be chosen based on other principles than the diffusion of solution species in chalcopyrite reaction product layer. In several studies [13,16,17], chemical or surface processes have been suggested to limit chalcopyrite concentrate dissolution in cupric chloride solutions. If the effect of the reaction product layer as a diffusion barrier is neglected, it could be suggested that the resistance for the chemical reactions at the chalcopyrite - solution or at the reaction product layer – solution

interface, is lower at pH 3 than at pH 1. This may be due to the formation of FeOOH, which pushes the equilibrium of dissolution reactions (1), (6) and (7) to the right. FeOOH can also have an effect by preventing the formation of a metal-deficient, dissolution hindering reaction product layer. The chalcopyrite dissolution rate increases gradually when increasing the pH from 1 to 3. It is clear that the HydroCopper® process cannot be run at pH 3 due to atacamite precipitation. However, even a slight increase in the operating pH values can increase chalcopyrite dissolution rates.

The cupric ion species was not identified unambiguously. However, calculations with HSC thermodynamic software suggested that the theoretical redox potential of solution was closest to the experimental redox potential (0.76 – 0.95 V vs. SHE) when the cupric ion was not complexed with chloride ions [42]. Recently published calculations using the MTAQ database [43] also support this hypothesis. Thus it was suggested that in concentrated cupric chloride solutions, Cu^{2+} could remain at least partially as hexa-aqua copper and not in a chloro-complex form.

A wide set of redox measurements was carried out in order to study the redox potentials of cupric chloride solutions as well as to find the E^o of the cathodic reaction. In a concentrated cupric chloride solution without additives, E^o was 0.158 V ± 0.121 V vs. SHE. This indicated that at very low concentrations (in the order of 10^{-15} mol/m^3) cuprous ions could remain uncomplexed i.e. they were not complexed with chloride ions. In the chemical environment studied the prevailing cuprous complex was suggested to be $[CuCl_3]^{2-}$, based on HSC 5.11/6.1 calculations, literature survey and novel calculations with the MTAQ database [43]. The conclusion that cuprous ions can stay in a non chloro-complex form at very low concentrations was thermodynamically interesting in the field of chloride complex thermodynamics. It is widely agreed that cuprous ions readily form chloro-complexes in more concentrated solutions. Also, the MTAQ database in *Figure 17* suggests that the prevailing cuprous species is a chloro-complex $[CuCl_3]^{2-}$. However, the results published in [IV] provide a new point of view on cuprous complexation at significantly low cuprous concentrations. These results may provide a tool for those building thermodynamic databases.

7 CONCLUSIONS

The target of this study was to observe chalcopyrite dissolution in cupric chloride solutions with high chloride concentrations. The research consisted of five reviewed and published [I] – [V] articles in the journals "Hydrometallurgy" and "Canadian Metallurgical Quarterly". These five articles presented the three main theses: (i) the nature of the reaction product layers forming on stationary chalcopyrite electrode, (ii) the rate limiting step for chalcopyrite dissolution and (iii) the prevailing cupric and cuprous species in concentrated cupric chloride solutions near the boiling point of the solution. The experimental techniques used were mainly electrochemical, but microscopy methods were also used.

It was observed that the formation and composition of the reaction product layer was strongly dependent on pH. At lower pHs, near to 1, a gray single-phase elemental sulfur layer formed at $t \leq 9$ h. With longer leaching times ($t > 9$ h), a two-phase layer of elemental sulfur and FeOOH was formed. The layer at pH 1 hindered the dissolution of chalcopyrite during the early hours more than the reaction product layer at higher pHs, close to pH 3. The layer at pH 1 was ca. 9 µm thick after 22 h of leaching. The resistance for chemical reactions at solid-solution interface at pH 1 increased at $t \leq 3$ h and decreased at $t > 3$h. At pH 2, the layer was a one-phase elemental sulfur in the early hours ($t<3$ h), but the second phase, FeOOH, was observed after longer dissolution times. The resistance for reactions at the solid – solution interface decreased with increasing time. The thickness of this layer was ca. 10 µm after 22 hours of leaching. At higher pHs, near to pH 3, a yellow-orange FeOOH-sulfur reaction product layer formed. Two phases were present at all times, up to 22 hours. The thickness of this layer was ca. 14 µm after 22 hours of leaching. The layer at pH 3 allowed faster chalcopyrite dissolution during early hours and also had a lower resistance for chemical reactions. The resistance for reactions on the solid - solution interface was low (~150 Ωcm^2) at all pHs and leaching times, compared to some other reaction product layers found in the literature.

The leaching mechanisms at pH 1 and at pH 3 were suggested. It was concluded that at low pHs and short leaching times a layer rich in elemental sulfur forms. This layer increases the resistance at the reaction product layer – solution interface, probably affected by the increase in the ferrous and ferric concentrations near the chalcopyrite surface. The dissolution rate is lower than at pH 3. By increasing the pH and time, FeOOH precipitated in addition to elemental sulfur. The precipitation of FeOOH pushed the reduction reaction of cupric by ferrous ions to the right, which in turn shifted the chalcopyrite leaching reaction to the right. FeOOH precipitation with an increasing pH made chalcopyrite dissolution more favorable than the formation of elemental sulfur alone.

It was shown that the cathodic reduction reaction rate did not limit the chalcopyrite dissolution. Nor did the diffusion in the solution limit the dissolution rate. EIS measurements confirmed that the resistance for chemical reactions in the reaction product layer – solution interface did not control chalcopyrite dissolution at higher pHs. Activation energies calculated showed that a phenomenon related to diffusion was the rate-limiting step at pH 2. Potentiostatic curves showed parabolic kinetics at pH 3 turning into inverse parabolic at pH 1. Thus it was concluded that the chalcopyrite electrode dissolution was limited by the diffusion

of cathodic reactants through the reaction product layer at pH 3. At pH 1 the dissolution was limited more by the anodic dissolution reaction rate.

The prevailing cupric and cuprous species were studied experimentally. In concentrated cupric chloride solution without additives E^o was 0.158 V ± 0.121 V vs. SHE. This showed that in such low concentrations (in the order of 10^{-15} mol/m^3) cuprous ions can remain uncomplexed, i.e. they are not complexed with chloride ions. At higher cuprous concentrations, the prevailing cuprous complex was suggested to be $[CuCl_3]^{2-}$, based on HSC 5.11 calculations, literature survey and recent calculations with MTAQ-database [43]. The form of cupric ion could not be specified, however, thermodynamic observations with HSC 5.11 suggested that the theoretical redox potential of the solution is closer to the experimental redox potential when cupric ion is not complexed with chloride ions. Recently published calculations with the MTAQ database [43] also support this idea. Thus it is suggested that cupric ions can be present in chloride media as a species without being complexed with chloride ions.

8 REFERENCES

[1] A.R. Burkin, Chemical Hydrometallurgy, Theory and Principles. Singapore, Imperial College Press, (2001) pp.12, 364-373.

[2] E.M. Córdoba, J.A. Munoz, M.L. Blazquez, F. Gonzalez, and A. Ballester, Leaching of Chalcopyrite with Ferric Ion. Part I: General Aspects. Hydrometallurgy 93(2008), pp. 81-87.

[3] F. Habashi, Chalcopyrite its Chemistry and Metallurgy, ed. British Library Cataloging (1978). Chatham, McGraw-Hill, pp. 165.

[4] J. Peacey, X.J. Guo, and E. Robles, Copper Hydrometallurgy - Current Status, Preliminary Economics, Future Direction and Positioning versus Smelting. Transactions of the Nonferrous Metals Society of China 14(2004) 3, pp. 560-568.

[5] D. Dreisinger, Copper Leaching from Primary Sulfides: Options for Biological and Chemical Extraction of Copper. Hydrometallurgy 83(2006) 3-4, pp. 10-20.

[6] D.S. Flett, Chloride Hydrometallurgy for Complex Sulphide: A review. CIM Bulletin 95(2002) 1065, pp. 65-73.

[7] R.P. Hackl, D.P. Dreisinger, E. Peters, and J.A. King, Passivation of Chalcopyrite During Oxidative Leaching in Sulfate Media. Hydrometallurgy 39(1995) 1, pp. 25-48.

[8] R. Padilla, P. Zambrano, and M.C. Ruiz, Leaching of Sulfidized Chalcopyrite with H_2SO_4-NaCl-O_2. Metallurgical and Materials Transactions 34B(2003), pp.153-158.

[9] R.J. Roman and B.R. Benner, The Dissolution of Copper Concentrates. Minerals Science and Engineering 5(1973) 1, pp. 3-24.

[10] H.K. Lin, Characterization and Flotation of Sulfur from Chalcopyrite Concentrate Leaching Residue. Journal of Minerals & Materials Characterization & Engineering 2(2003) 1, pp. 1-9.

[11] E.F.G. Milner, E. Peters, G.M. Swinkels, and A.I. Vizsolyi, Copper Hydrometallurgy. In *US3798026* (1974), Cominco Ltd, Canada.

[12] M. Skrobian, T. Havlik, and M. Ukasik, Effect of NaCl Concentration and Particle Size on Chalcopyrite Leaching in Cupric Chloride Solution. Hydrometallurgy 77(2005), pp. 109-114.

[13] J.P. Wilson and W.W. Fisher, Cupric Chloride Leaching of Chalcopyrite. Journal of Metals 33(1981) 2, pp. 52-57.

[14] J. Liddicoat and D. Dreisinger, Chloride Leaching of Chalcopyrite. Hydrometallurgy 89(2007), pp. 323-331.

[15] M. Al-Harahsheh, S. Kingman, and A. Al-Harahsheh, Ferric Chloride Leaching of Chalcopyrite: Synertic Effect of $CuCl_2$. Hydrometallurgy 91(2008) 89-97.

[16] T. Hirato, H. Majima, and Y. Awakura, The Leaching of Chalcopyrite with Cupric Chloride. Metallurgical Transactions 18B(1987), pp. 31-39.

[17] M. Bonan, J.M. Demarthe, H. Renon, and F. Baratin, Chalcopyrite Leaching by $CuCl_2$ in Strong NaCl Solutions. Metallurgical Transactions 12B(1981), pp. 269-274.

[18] L. Haavanlammi, K. Hietala, and J. Karonen, HydroCopper® for Treating Variable Copper Concentrates. In The John E. Dutrizac International Symposium on Copper Hydrometallurgy (2007), Toronto, Canada, CIM, pp.369-377.

[19] L. Haavanlammi, J. Karonen, and C. Rodriquez, HydroCopper® - Moving Up in the Copper Production Chain. In First International Workshop on Process Hydrometallurgy, 11-13th October (2006), Iquique, Chile.

[20] K. Hietala and O. Hyvärinen, HydroCopper™ - A New Technology for Copper Production. In Alta 2003 Copper Conference (2003), Perth, Australia, pp.1-10.

[21] O. Hyvärinen, HydroCopper™ - Outokummun Käänteentekevä Uusi Kuparinvalmistusmenetelmä. Vuoriteollisuus - Bergshanteringen 3(2003), pp. 49-52.
[22] O. Hyvärinen, M. Hämäläinen, P. Lamberg, and J. Liipo, Recovering Gold from Copper Concentrate via the HydroCopper™ Process. JOM 56(2004) 8, pp. 57-59.
[23] O. Hyvärinen, M. Hämäläinen, and R. Leimala, Outokumpu HydroCopper™ Process A Novel Concept in Copper Production. In Chloride Metallurgy 2002, 32nd Annual Hydrometallurgy Meeting (2002), Montreal, Quebec, Canada, MetSoc of CIM, pp.609-612.
[24] P. Sinisalo, M. Tiihonen, and K. Hietala, Gold Recovery from Chalcopyrite Concentrates in the HydroCopper® Process. In ALTA 2008 Conference, June 19-20, (2008), Perth, Australia, pp. 1-8.
[25] T. Kekesi and M. Isshiki, Anion Exchange for the Ultra-High Purification of Transition Metals. Erzmetall 56(2003) 2, pp. 59-67.
[26] Z.Y. Lu, M.I. Jeffery, and F. Lawson, The Effect of Chloride Ions on the Dissolution of Chalcopyrite in Acidic Solutions. Hydrometallurgy 56(2000), pp. 189-202.
[27] R. Winand, Chloride Hydrometallurgy. Hydrometallurgy 27(1991), pp. 285-316.
[28] D.M. Muir. Basic Principles of Chloride Hydrometallurgy. In Chloride Metallurgy 2002, 32nd Annual Hydrometallurgy Meeting (2002), Montreal, Canada, MetSoc, pp. 759-778.
[29] J.E. Dutrizac, The Kinetics of Dissolution of Chalcopyrite in Ferric Ion Media. Metallurgical Transactions 9B(1978), pp. 431-439.
[30] J.M. Berger and R. Winand, Solubilities, Densities and Electrical Conductivities of Aqueous Copper(I) and Copper(II) Chlorides in Solutions Containing Other Chlorides such as Iron, Zinc, Sodium and Hydrogen Chlorides. Hydrometallurgy 12(1984), pp. 61-81.
[31] H. Stephen and T. Stephen, Solubilities of Inorganic and Organic Compounds, Vol. 1, Binary Systems, Part 1 (1963), London, Pergamon Press, pp.14,15,184, 185
[32] C. Christov, Thermodynamic Study of the Na-Cu-Cl-SO_4-H_2O System at the Temperature 298.15 K. Journal of Chemical Thermodynamics 32(2000), pp. 285-295.
[33] M.D. Collins, D.M. Sherman, and K.V. Ragnarsdottir, Complexation of Cu^{2+} in Oxidized NaCl Brines from 25 °C to 175 °C: Results from in situ EXAFS Spectroscopy. Chemical Geology 167(2000), pp. 65-73.
[34] A. Fontana, J. van Muylder, and R. Winand, Etude Spectrophotometrique de Solutions Aqueuses Chlorurees de Chlorure Cuivreux, a Concentrations Elevees. Hydrometallurgy 11(1983), pp. 287-314.
[35] J.J. Fritz, Chloride Complexes of CuCl in Aqueous Solution. Journal of Physical Chemistry 84(1980) 18, pp. 2241-2246.
[36] T. Salo, The Electrochemical Properties of Copper Chloride Electrolyte. Master´s Thesis in Materials Science and Rock Engineering (1995), Helsinki University of Technology, Espoo. p. 32.
[37] Z. Xiao, C.H. Gammons, and A.E. Williams-Jones, Experimental Study of Copper(I) Chloride Complexing in Hydrothermal Solutions at 40 to 300ºC and Saturated Water Vapor Pressure. Geochimica et Cosmochimica Acta 62(1998) 17, pp. 2949-2946.
[38] H.-H. Haung, Estimation of Pitzer´s Ion Interaction Parameters for Electrolytes Involved in Complex Formation Using a Chemical Equilibrium Model. Journal of Solution Chemistry 18(1989) 11, pp. 1069-1085.
[39] J.J. Fritz, Determination of Equilibrium Constants for Complex Species Formed from Slightly Soluble Salts. The Journal of Physical Chemistry 88(1984) 19, pp. 4358-4361.

[40] L. Ciavatta and M. Iuliano, Copper(I) Chloride Complexes in Aqueous Solution. Societa Chimica Italiana 88(1998), pp. 71-89.
[41] J.J. Fritz, Representation of the Solubility of CuCl in Solutions of Various Aqueous Chlorides. The Journal of Physical Chemistry 85(1981) 7, pp. 890-894.
[42] M. Lundström, J. Aromaa, O. Forsén, and L. Haavanlammi, Concentrated Cupric Chloride Solutions: Possibilities Offered in Copper Production. Acta Metallurgica Slovaca 13(2007) 3, pp. 447-459.
[43] J. Pihlasalo, H. Davies, and P.A. Taskinen, Validation of a new Pitzer Type Model and Database for Aqueous Solutions with Outotec HydroCopper™ Process Data. In *CALPHAD 2008*, Saariselkä, Finland.
[44] V.M.M. Lobo and J.L. Quaresma. Handbook of Electrolyte Solutions Part B (1989), Coimbra, Portugal, Elsevier, pp. 377, 1603, 1615.
[45] T. Havlik and R. Kammel. Behavior of Sulfur During Leaching of Sulfide Mineral. In TMS Annual Meeting, February 4-9 (1996), Anaheim, California, TMS.
[46] R. von Bonsdorff, Dissolution of Gold in Cupric Chloride Solution. Master´s Thesis in Department of Materials Science and Rock Engineering (2004), Helsinki University of Technology, Espoo. p. 69.
[47] L. Haavanlammi, HydroCopper® Process. In Hydrometallurgy Short Course, Copper - Cobre 2007, Toronto, MetSoc of CIM.
[48] J. Karonen, HydroCopper™ Process. In Thermodynamic and Kinetic Phenomena in Hydrometallurgical Processes (2006), Espoo, Helsinki University of Technology, TKK-MT-182.
[49] R. von Bonsdorff, N. Järvenpää, J. Aromaa, O. Forsén, O. Hyvärinen, and M.H. Barker, Electrochemical Sensors for the HydroCopper™ Process Solution. Hydrometallurgy 77(2005), pp. 155-161.
[50] M. Lundström, Leaching of Chalcopyrite in Cupric Chloride Media. Master´s Thesis in Materials Science and Rock Engineering (2004), Helsinki University of Technology, Espoo. pp. 97.
[51] M. Lundström, Simulation of Cathodic Reactions in Cupric Chloride Solution. Licentiate Thesis in Department of Material science and Engineering (2007), Helsinki University of Technology, Espoo, pp. 102.
[52] M. Lundström, J. Aromaa, O. Forsén, and M.H. Barker. Reaction Product Layer on Chalcopyrite in Cupric Chloride Leaching. In The John E. Dutrizac International Symposium on Copper Hydrometallurgy (2007), Toronto, Canada, MetSoc of CIM, pp. 209-219.
[53] A.J. Bard and L.R. Faulkner, Electrochemical Methods Fundamentals and Applications. 2 ed (2001), John Wiley & Sons. inc. pp. 239-241, 335, 337, 347.
[54] Bernard A. Boukamp, Equivalent Circuit (Equivcrt.pas), University of Twente, (1988/89), Enschede, Netherlands.
[55] N. Hiroyoshi, S. Kuroiwa, H. Miki, M. Tsunekawa, and T. Hirajima, Synergistic Effect of Cupric and Ferrous Ions on Active-Passive Behavior in Anodic Dissolution of Chalcopyrite in Sulfuric Acid Solutions. Hydrometallurgy 74(2004), pp. 103-116.
[56] P.H.-M. Kinnunen, S. Heimala, M.-L. Riekkola-Vanhanen, and J.A. Puhakka, Chalcopyrite Concentrate Leaching with Biologically Produced Ferric Sulphate. Bioresource Technology 97(2006), pp. 1727-1734.
[57] D. Dreisinger. New Developments in the Leaching of Base and Precious Metal Ores and Concentrates. In XXII International Mineral Processing Congress (2003), Cape Town, South Africa, The South African Institute of Mining and Metallurgy.

[58] A. Parker, C. Klauber, A. Kougianos, H.R. Watling, and W. van Broswijk, An X-ray Photoelectron Spectroscopy Study of the Mechanism of Oxidative Dissolution of Chalcopyrite. Hydrometallurgy 71(2003) 1-2, pp. 265-276.

[59] J.E. Dutrizac and P.A. Riveros, The Precipitation of Hematite from Ferric Chloride Media at Atmospheric Pressure. Metallurgical and Materials Transactions 30B(1999), pp. 993-1001.

[60] P.A. Riveros and J.E. Dutrizac, The Precipitation of Hematite From Ferric Chloride Media. Hydrometallurgy 46(1997), pp. 85-104.

[61] T. Havlík, M. Skrobian, P. Baláz, and R. Kammel, Leaching of Chalcopyrite Concentrate with Ferric Chloride. International Journal of Mineral Processing 43(1995), pp. 61-72.

[62] T. Havlík and R. Kammel, Leaching of Chalcopyrite with Acidified Ferric Chloride and Carbon Tetrachloride Addition. Mineral Engineering 8(1995) 10, pp. 1125-1134.

[63] Y.L. Mikhlin, Y.V. Tomashevich, I.P. Asanov, A.V. Okotrub, V.A. Varnek, and D.V. Vyalikh, Spectroscopic and Electrochemical Characterization of the Surface Layers of Chalcopyrite ($CuFeS_2$) Reacted in Acidic Solutions. Applied Surface Science 225(2004), pp. 395-409.

[64] J.E. Dutrizac, Elemental Sulphur Formation During the Ferric Chloride Leaching of Chalcopyrite. Hydrometallurgy 23(1990), pp. 153-176.

[65] G.K. Parker, Spectroelectrochemical Investigation of Chalcopyrite Leaching. Doctoral Thesis in Faculty of Science (2005), Griffith University. pp. 98,99,131.

[66] B.R. Palmer, C.O. Nebo, M.F. Rau, and M.C. Fuerstenau, Rate Phenomena Involved in the Dissolution of Chalcopyrite in Chloride-Bearing Lixiviants. Metallurgical Transactions 12B(1981), pp. 595-561.

[67] A.C. Scheinost and U. Schwertmann, Color Identification of Iron Oxides and Hydroxysulfates: Use and Limitations. Soil Science Society of America Journal 63(1999), pp. 1463-1471.

[68] T. Cabral and I. Ignatiadis, Mechanistic Study of the Pyrite-Solution Interface During the Oxidative Bacterial Dissolution of Pyrite (FeS_2) by Using Electrochemical Techniques. International Journal of Mineral Processing 62(2001), pp. 41-64.

[69] D. Bevilaqua, I. Diéz-Perez, C.S. Fugivara, F. Sanz, A.V. Benedetti, and O. Garcia Jr, Oxidative Dissolution of Chalcopyrite by Acidithiobacillus Ferrooxidans Analyzed by Electrochemical Impedance Spectroscopy and Atomic Force Microscopy. Bioelectrochemistry 64(2004), pp. 79-84.

[70] P. Velásquez, E. Gómez, D. Leinen, and J.R. Ramos-Barrado, Electrochemical Impedance Spectroscopy Analysis of Chalcopyrite $CuFeS_2$ Electrodes. Colloids and Surfaces 140(1998), pp. 177-182.

[71] P. Velásquez, et al., XPS, SEM, EDX and EIS Study of an Electrochemically Modified Electrode Surface of Natural Chalcocite (Cu_2S). Journal of Electroanalytical Chemistry 510(2001), pp. 20-28.

[72] S.-y. Shi, Z.-h. Fang, and J.-r. Ni, Electrochemical Impedance Spectroscopy of Marmatite-Carbon Paste Electrode in the Presence and Absence of Acidithiobacillus Ferrooxidans. Electrochemistry Communications 7(2005), pp. 1177-1182.

[73] P. Nowak and A. Gucwa, Influence of Surfactant Adsorption on the Leaching of Copper Sulfides. Acta Metallurgica Slovaca 14(2008), pp. 196-203.

[74] R.G. Kelly, J.R. Scully, D.W. Shoesmith, and R.G. Buchheit, Electrochemical Techniques in Corrosion Science and Engineering, ed. M. Dekker (2003), New York, Basel.

[75] R. Cabrera-Sierra, I. García, E. Sosa, T. Oropeza, and I. González, Electrochemical Behavior of Carbon Steel in Alkaline Sour Environments Measured by

Electrochemical Impedance Spectroscopy. Electrochimica Acta 46(2000), pp. 487-497.

[76] E. Peters. The Physical Chemistry of Hydrometallurgy. AIME International Symposium on Hydrometallurgy (1973), Chicago, February, pp.205-258.

[77] J.E. Dutrizac, The Dissolution of Chalcopyrite in Ferric Sulfate and Ferric Chloride Media. Metallurgical Transactions 12B(1981), pp. 371-378.

[78] J.E. Dutrizac, Ferric Ion Leaching of Chalcopyrites from Different Localities. Metallurgical Transactions 13B(1982), pp. 303-309.

[79] E. Godociková, P. Baláz, and E. Boldizárová, Structural and Temperature Sensitivity of the Chloride Leaching of Copper, Lead and Zinc from a Mechanically Activated Complex Sulphide. Hydrometallurgy 65(2002), pp. 83-93.

[80] T. Kekesi and M. Isshiki, Electrodeposition of Copper from Pure Cupric Chloride Hydrochloric Acid Solutions. Journal of Applied Electrochemistry 27(1997) 8, pp. 982-990.

[81] D.G. Winter, J.W. Covington, and D.M. Muir, Studies Related to the Electrowinning of Copper from Chloride Solutions. In 111th AIME Annual Meeting, February (1982), Dallas, Texas, AIME TMS, pp.167-188.

[82] D.P. Gregory and A.C. Riddiford, Transport to the Surface of a Rotating Disc. Journal of the Chemical Society, (1956), pp. 3756-3764.

[83] W. Liu, D.C. McPhail, and J. Brugger, An Experimental Study of Copper(I)-Chloride and Copper(I)-Acetate Complexing in Hydrothermal Solutions Between 50 °C and 250 °C and Vapor-Saturated Pressure. Geochimica et Cosmochimica Acta 65(2001) 17, pp. 2937-2948.

[84] G.K. Parker, R. Woods and G.A. Hope, Raman Investigation of Chalcopyrite Oxidation. Colloids and Surfaces A 318(2008), pp. 160-168.

[85] A.N. Buckley, H.J. Wouterlood and R. Woods, The Surface Composition of Natural Sphalerites Under Oxidative Leaching Conditions. Hydrometallurgy 22(1989), pp. 39-56.

Appendix 1. *A cross cut SEM picture of an electrode made at Outotec Research Oy after anodic polarization at pH 3. The solution had [NaCl] = 250 g/L, [Cu^{2+}] = 17.9 g/L, T = 85 ºC.*

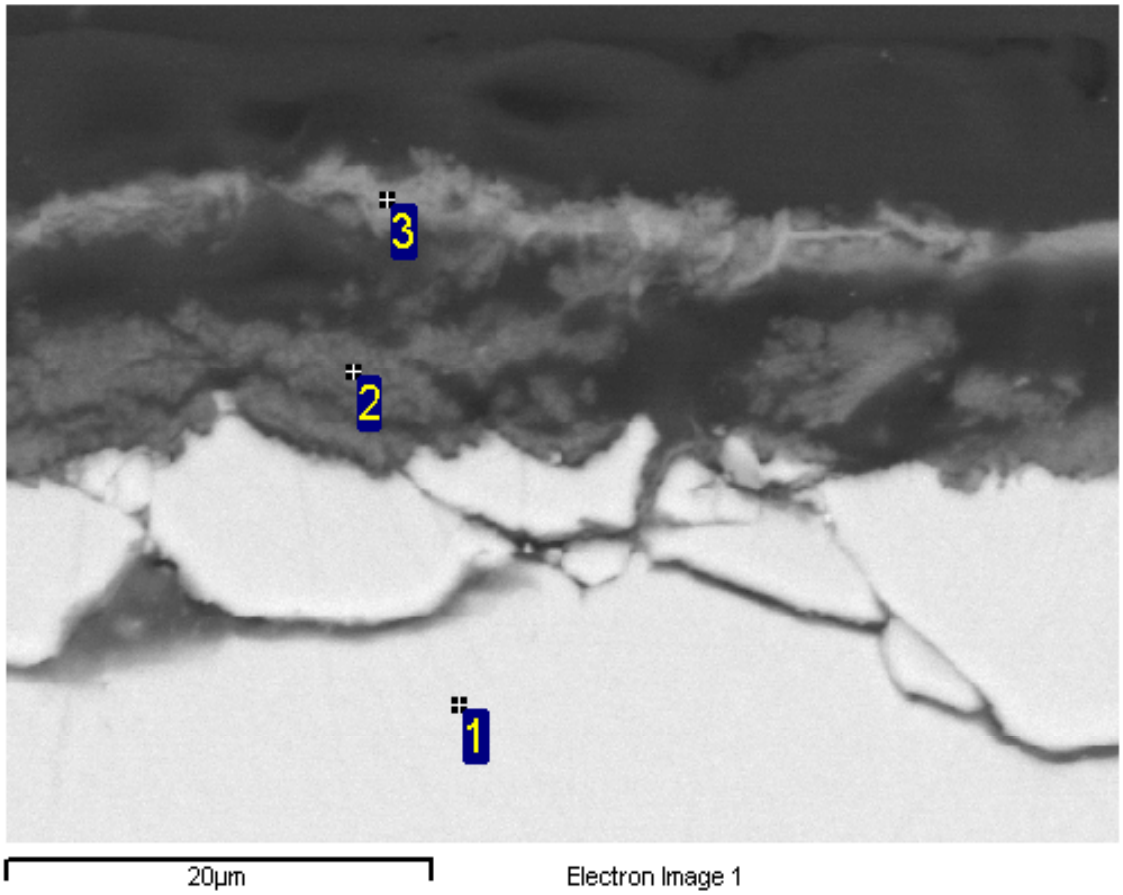

Processing option : All elements analyzed (Normalized)

Spectrum	O	Si	P	S	Cl	Fe	Cu	Total
1				35.96		30.89	33.15	100.00
2	32.64	0.76		3.22	9.99	53.39		100.00
3	37.52	1.52	0.44	2.50	7.80	50.23		100.00

All results in Weight Percent

Appendix 2. *A closer analysis of the polished chalcopyrite electrode in Figure 8. The compositions of all points are shown in weight percent.*

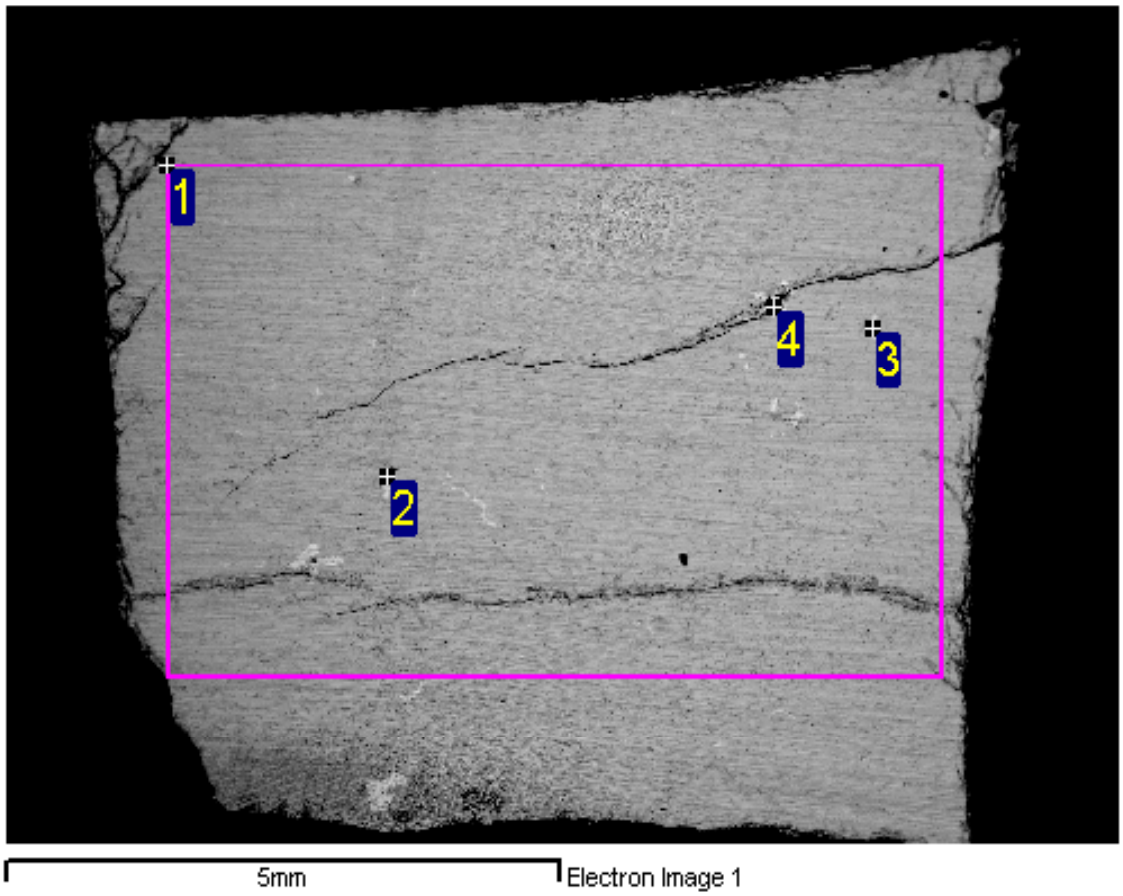

Processing option : All elements analyzed (Normalized)

Spectrum	S	Mn	Fe	Cu	Zn	Total
1	36.10		30.00	33.21	0.69	100.00
2	34.64	0.42	8.11	1.16	55.68	100.00
3	34.41	0.51	12.31	7.21	45.56	100.00
4	34.52	0.34	7.48	0.68	56.97	100.00

All results in Weight Percent

Appendix 3. *A closer analysis of the leached (pH 1.5) chalcopyrite electrode in Figure 8. The compositions of all points are shown in weight percent.*

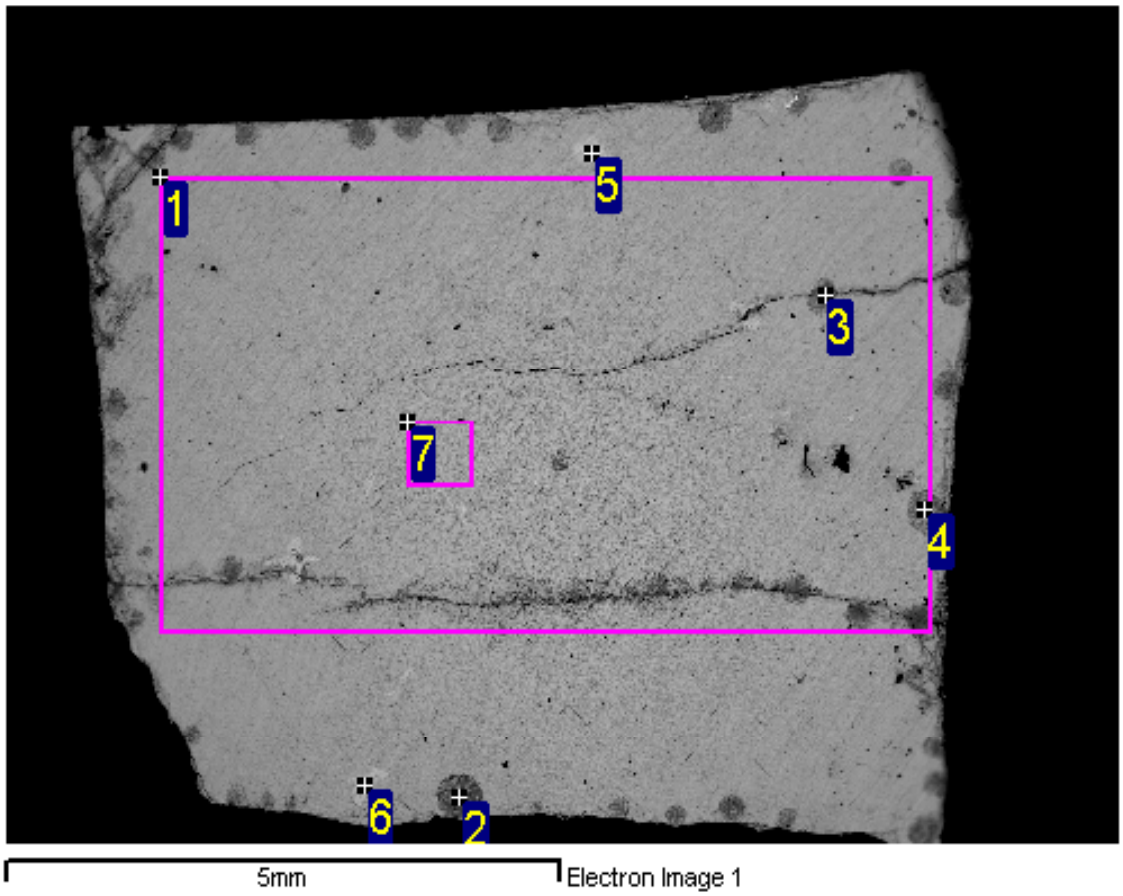

Processing option : All elements analyzed (Normalized)

Spectrum	O	Na	Si	S	Cl	Mn	Fe	Cu	Zn	Ag	Total
1				38.12			29.60	32.28			100.00
2	22.31	1.82		22.90	9.35		28.88	14.73			100.00
3	21.31			19.68	4.18		36.32	18.51			100.00
4	17.62			23.31	4.23		33.53	21.31			100.00
5				35.61			28.55	31.02		4.83	100.00
6			0.03	37.37		0.46	6.93		55.22		100.00
7			0.01	37.26			30.03	32.69			100.00

All results in Weight Percent

Appendix 4. *A closer analysis of the leached (pH 3.0) chalcopyrite electrode in Figure 8. The compositions of all points are shown in weight percent.*

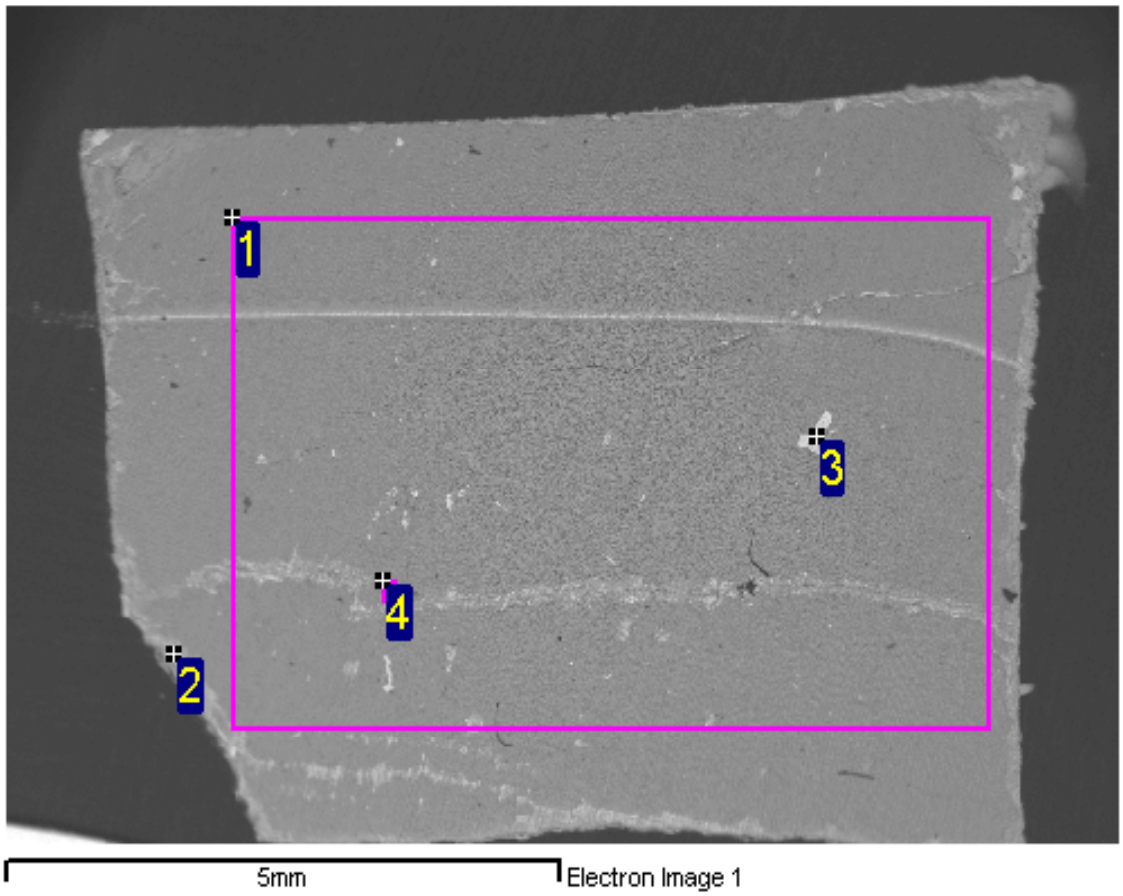

Processing option : All elements analyzed (Normalized)

Spectrum	O	P	S	Cl	Fe	Cu	Zn	Total
1	21.41		38.76	3.74	33.61	2.48		100.00
2	22.50		23.27	5.97	34.12	14.14		100.00
3	3.61		33.64		7.88		54.87	100.00
4	17.88	0.55	30.62	2.79	33.42	14.75		100.00

All results in Weight Percent

Appendix 5. *XRD spectrum and analysis of the chalcopyrite reaction product layer after leaching at pH 1 for 22 hours at OCP.*

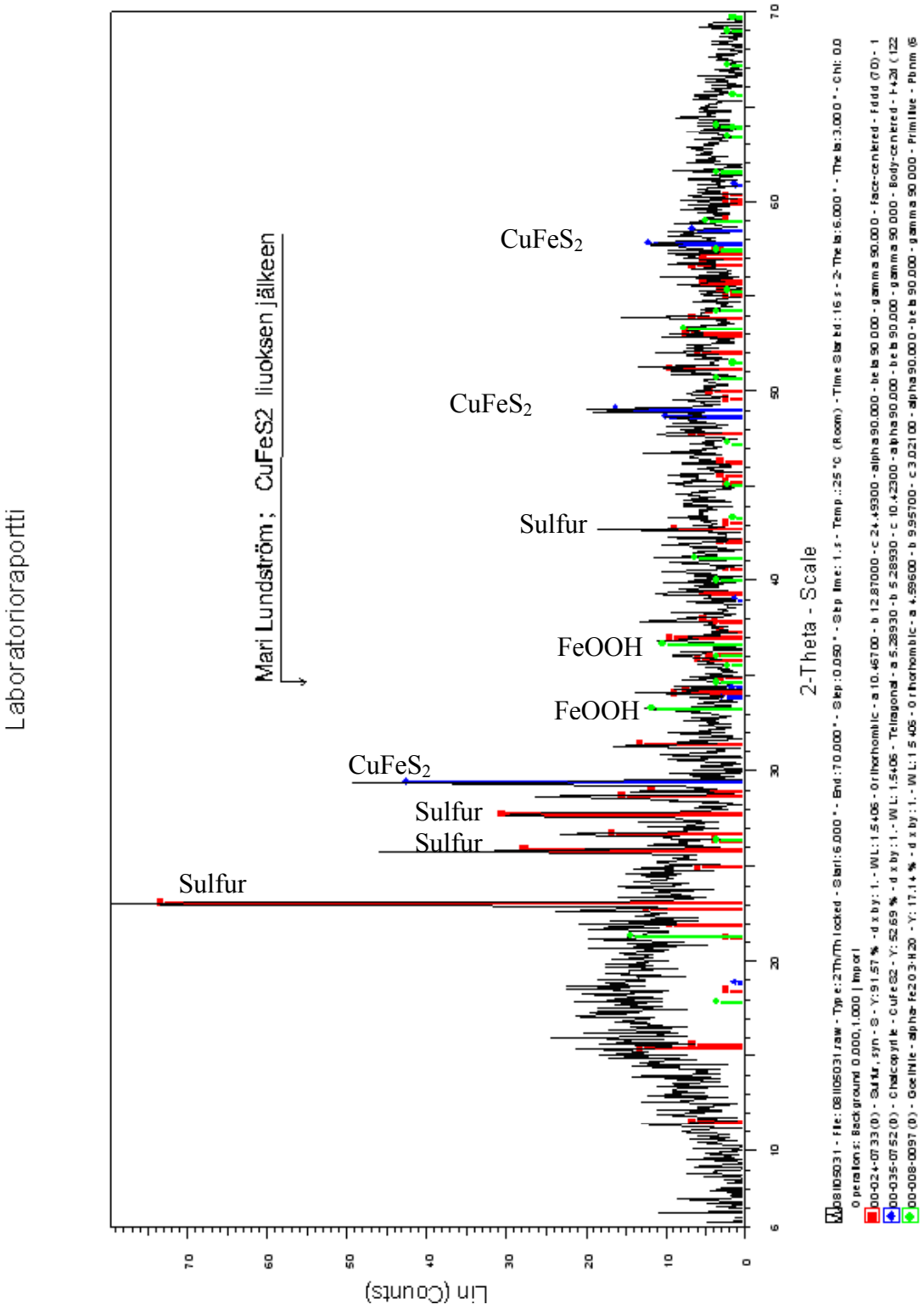

Appendix 6. *XRD spectrum and analysis of the chalcopyrite reaction product layer after leaching at pH 2 for 22 hours at OCP.*

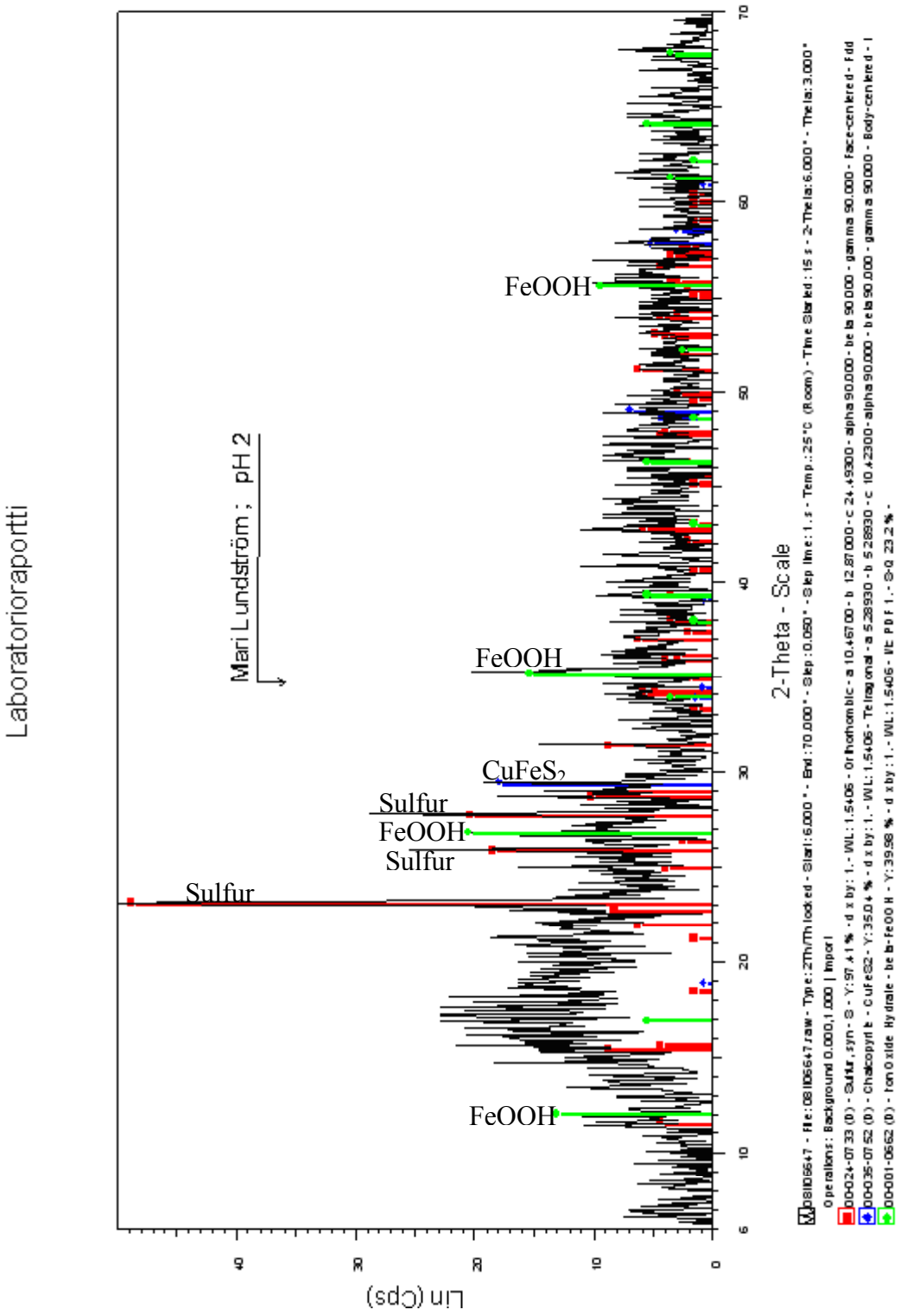

Appendix 7. *XRD spectrum and analysis of the chalcopyrite reaction product layer after leaching at pH 3 for 22 hours at OCP.*

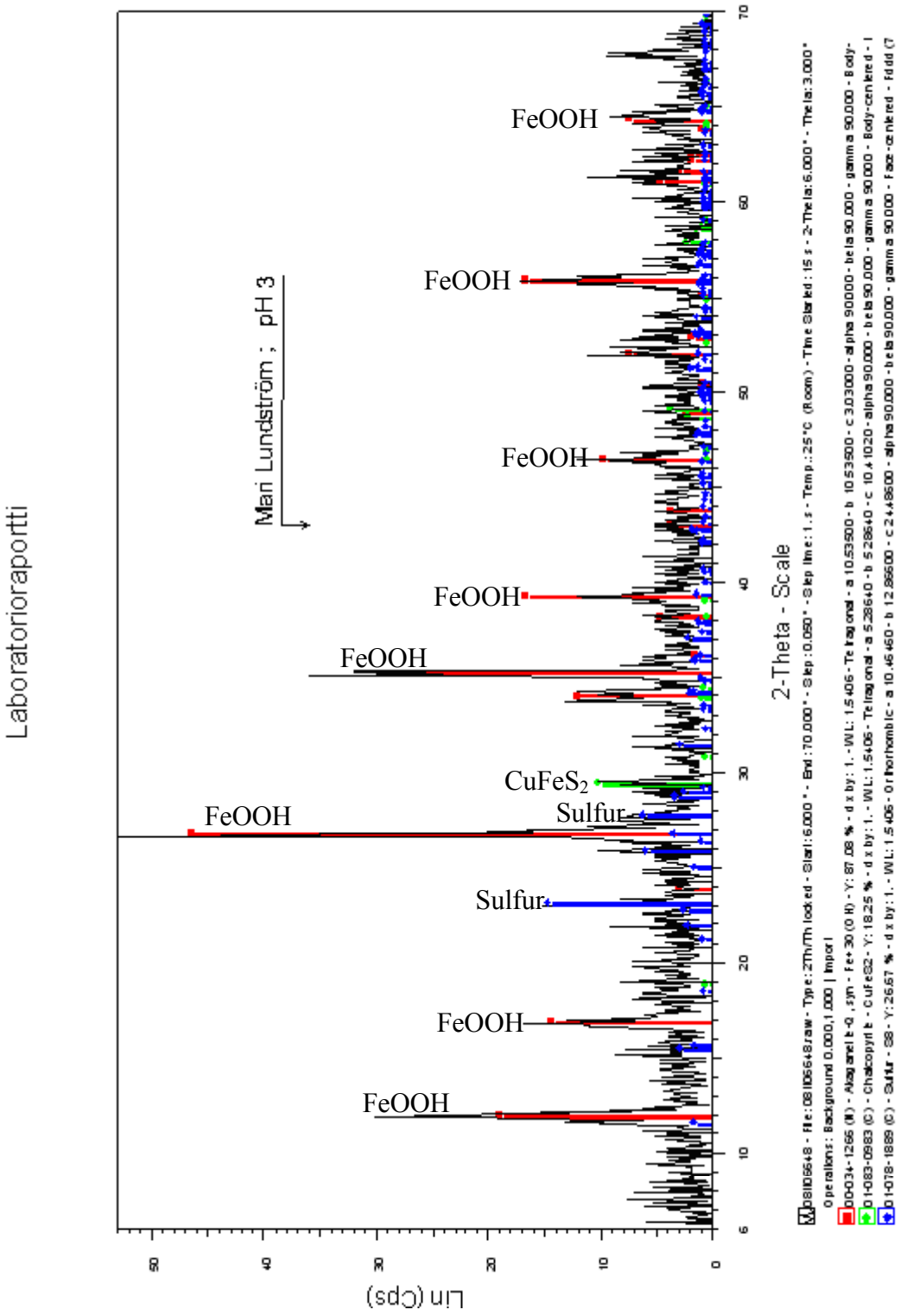

HELSINKI UNIVERSITY OF TECHNOLOGY DOCTORAL THESES IN MATERIALS AND EARTH SCIENCES

TKK-ME-DT-1 Ranki-Kilpinen, T.,
Sulphation of Cuprous and Cupric Oxide Dusts and Heterogeneous Copper Matte Particles in Simulated Flash Smelting Heat Recovery Boiler Conditions. 2004

TKK-ME-DT-2 Söderberg, O.,
Novel Ni-Mn-Ga Alloys and their Magnetic Shape Memory Behaviour. 2004

TKK-ME-DT-3 Kaskiala, T.,
Studies on Gas-Liquid Mass Transfer in Atmosperic Leaching of Sulphidic Zinc Concentrates. 2005

TKK-ME-DT-4 Grau, R.A.,
An Investigation of the Effect of Physical and Chemical Variables on Bubble Generation and Coalescence in Laboratory Scale Flotation Cells. 2006

TKK-ME-DT-5 Kivikytö-Reponen, P.,
Correlation of Material Characteristics and Wear of Powder Metallurgical Metal Matrix Composites. 2006

TKK-ME-DIS-6 Ge, Y.,
The Crystal and Magnetic Microstructure of NI-Mn-Ga Alloys. 2007

TKK-ME-DIS-7 Kankaanpää, T.,
CFD Procedure for Studying Dispersion Flows and Design Optimization of the Solvent Extraction Settler. 2007

TKK-ME-DIS-8 Miettinen, E.,
Thermal Conductivity and Characteristics of Copper Flash Smelting Flue Dust Accretions. 2008

ISBN 978-951-22-9937-9
ISBN 978-951-22-9938-6 (electronic)
ISSN 1795-0074